REVIEW PAPER

THE HIGH PRESSURE GAS TURBINE BLADES OF JET ENGINES

R. Prabhakaran
Eminent Professor
Department of Mechanical and Aerospace Engineering
Old Dominion University
Norfolk, VA 23529, U S A
Email : rprabhak@odu.edu

Abstract

The modern turbo-engine is one of the finest examples of engineering ingenuity, complexity and usefulness. The turbo-engine, whether used in land-based power generating equipment or in aircraft propulsion, has had a profound impact on our lives. Increasing air-travel, rising fuel prices, and environmental concerns have all combined to increase the need for more fuel-efficient engines. The blades of the high-pressure turbine are the most severely loaded members in the turbo-engine. The various aspects of these blades are described. First, the major components of a turbo-engine as well as the different types of turbo-engines are briefly described. Then the development of the turbo-engine is placed in its historical perspective. Next, the severity of the blade loading conditions, such as high temperatures, high centrifugal stresses, corrosion, oxidation, sulphidation, foreign object damage, etc., and the resulting failure modes are summarized. Super alloys are the materials of choice for these blades. The incremental improvements in the alloy chemistry are briefly traced. Important developments in the blade manufacture, the different types of blade cooling channels and their machining, thermal barrier coatings to decrease the blade temperature while increasing the Turbine Inlet Temperature (TIT), and future trends are discussed. The future belongs inevitably to advanced ceramics and their composites, with coatings for environmental protection.

Introduction

A gas-turbo-engine has five essential parts [Refs. 1, 2]: air intake, compressor, combustion chamber, turbine and exhaust as shown in Fig.1, [Ref.3]. The compressor, combustion chamber and turbine form the 'core' of the engine.

The air intake directs the air into the compressor. The compressor, driven by the turbine, increases the air pressure and sends the air into the combustion chamber. The compressor has many stages, each increasing the air pressure incrementally. In the combustion chamber, compressed air is mixed with the fuel and ignited. The combustion products are directed into the turbine. The turbine, in a land-based power generation plant, has several stages; it rotates the compressor and spins the generator which produces electricity. In a land-based gas turbine, the air intake and the exhaust are present but their design is not as critical as in an aircraft engine. In a turbo-engine used for aircraft propulsion, the turbine rotates the compressor and also generates some electricity to provide power for the auxiliary systems; but the major part of the energy in the combustion gases is used to generate the propulsive thrust as the gases exit through the exhaust nozzle.

There are four types of turbo-engines for aircraft: (i) In the turbo-jet engine, the first jet engine to be made, the turbine extracts some energy from the hot gases to drive the compressor and auxiliary systems but the exhaust gases generate the propulsive thrust when they exit the nozzle at high velocity. The turbo-jet is efficient mainly at high speeds, as in fighter or acrobatic aircraft. (ii) In the turbo-fan engine, there is an over-sized fan in the front, rotated by the turbine through a separate shaft at a slower speed. Most of the air through the fan bypasses the core of the engine and exits through the nozzle, generating additional thrust. The bypass engines were introduced in 1962 and marked a significant improvement for aero engines

Paper Code : V69 N2/959-2017. Manuscript received on 21 Sep 2016. Reviewed and accepted as a Review Paper on 05 Apr 2017

This Paper is dedicated to the Late Professor R. Srivatsavan, PSG College of Technology, Coimbatore, Tamil Nadu, India

(4). The "bypass ratio" is the ratio of the air that bypasses the engine core to the air that goes through the core of the engine. Current bypass ratios are five to one or more. The fan is surrounded by a cowl and generates 75 to 80 percent of the total thrust. The advantages of the turbo-fan engine are low noise levels and better fuel efficiency. (iii) In the turbo-prop engine, the turbine drives an over-sized propeller at slower speed. The air drawn in by the propeller generates more thrust than the exhaust gases exiting through the exhaust nozzle. Turbo-props are good for low speed aircraft, like commuter aircraft and cargo planes. (iv) Turbo-shaft engine generates shaft power instead of thrust. The shaft power is used to spin the rotor blades of a helicopter, or to drive a battle tank, a racing car or a cruise ship.

A Short History of Gas Turbo Engines

To understand the progress and the state of the art in any field, it is useful to briefly consider the historical developments. Concentrating on the major developments [Refs. 4-9], in 1930 Sir Frank Whittle, a cadet in the Royal Air Force in UK, patented his design for a jet engine in England. From 1934 to 1936, as he was enrolled at Cambridge University, he allowed his patent to lapse because the £5 patent renewal fee was not paid by the British Air Ministry [Refs.10,11]. In 1935, Hans von Ohain, a research student in Germany, unaware of Whittle's patent, got his own patent for a jet engine. The first jet engine with a liquid fuel was tested in England in 1937. Just weeks before the Second World War started, von Ohain's petroleum- fueled engine was fitted in a Heinkel He178 fighter plane shown in Fig.2 [Ref. 9] and was flown in Germany in 1939; this was the world's first aircraft to fly purely on turbo-jet power. Twenty months after that Whittle's engine was flown in England in a Gloster E28/29 experimental plane.

In 1940, the National Science Academy Committee on Gas Turbines in USA concluded that "there is no future for aircraft gas turbine engines", because after the turbine extracted the auxiliary power from the hot combustion gases, there would be very little energy left to generate the propulsive thrust! As part of the war effort, drawings of the Whittle's jet engine were given to the US government by the British government in 1941. In October 1941, a complete engine was given to General Electric (GE). The production of the engine started in US immediately after that. The early designs of aero engines of GE, Pratt & Whitney and Rolls Royce were based on Whittle's engine. Whittle emigrated to USA in 1976 and worked at GE to scale up the jet engines. Von Ohain, working for the German military during the Second World War, emigrated to USA in 1947 and became the Chief Scientist at the Wright-Patterson Air Force Base in Dayton, Ohio. In 1948, Chuck Yeager broke the sound barrier in a turbo-jet plane, X-1. In 1949, the first flight of a commercial turbo-jet aircraft, DH 106 Comet, took place.

Meanwhile attempts were made to apply the newly developed gas-turbine technology and gas turbo-jet technology in other fields [Refs.12-16]. In 1939, a 4 MW gas turbine was commissioned by Brown Boveri for power generation in Switzerland. It was operational until 2002! Gas turbine engines were used to power locomotives: in 1941, Brown Boveri's first locomotive with 1620 kW was delivered to Swiss Federal Railways and in 1951, Union Pacific Railroad commissioned a GE locomotive with 6300 kW which ran until 1969. The M-497 turbo-jet train in the USA (1966) and the SVL ER22 turbo-jet train in the USSR (1970) were attempts to introduce the turbo-jet technology to trains; but noise was one of the factors that terminated these experiments.

In 1947, Metrovick F-2 axial-flow jet engine in MGB 2009 became the first ever gas turbine propelled sea going vessel. In 1951, the first tanker powered by a gas turbine power plant, a 12000 tons DW tanker, "Auris", was commissioned by the Anglo Saxon Petroleum Company. These days cruise ships and sea going vessels routinely use turbo-engines. Among the land-based applications, battle tanks, BMW Panther tanks in 1944 and Swedish tanks in 1950 were the first vehicles to use turbo-engines. Rover JET 1 was the first car powered by a gas-turbine engine in 1950. In 1952, a French turbine powered car, the Socema-Gregoire, was displayed at the Paris auto show. The first turbine powered car in USA was Firebird I, built by General Motors. The car was built in the 1950s but only for testing and evaluation. Starting in1954 with a modified Plymouth, Chrysler (USA) demonstrated several prototype gas- turbine powered cars. Later Fiat, Toyota, Volvo, Jaguar and GM built gas-turbine powered cars. The fictional Batmobile is often said to be powered by a gas-turbine or a jet engine. Bloodhound Supersonic Car (SSC) is the name of a racing car built in UK to break the land speed record. Approximately half of the thrust of Bloodhound SSC is provided by a Eurojet EJ 200, a highly sophisticated military turbo-fan engine normally found in the engine bay of a Eurofighter, Typhoon. The rest of the power comes from a custom designed hybrid rocket. It has a design speed of 1609 km/hour (1050 mph). Buses and

motorcycles have also been designed and made with gas turbines.

Turbine Blade Loading Conditions and Failure Modes

In a turbo-engine, the high-pressure turbine blade is the most severely loaded member and therefore the most critical component because the high-pressure turbine is located right next to the combustion chamber. Therefore, as Fig.3 [Ref.12] shows, the pressure and temperature of the combustion products are the maximum when these gases impinge on the high pressure turbine blades. In addition, these blades rotate at several thousand rpm and thus the centrifugal stresses are high. The temperature is maximum at the blade tip and decreases towards the root, whereas the centrifugal stresses are the maximum at the root and decrease towards the tip.

The blades are subjected to various types of loads: centrifugal loads due to the blade rotation, thermal loads due to the thermal gradients and high temperatures, aerodynamic loads due to the impingement of the combustion gases and vibratory loads due to the vibrations.

The combination of high stresses and high temperatures can lead to yielding, creep elongation (causing contact with the stator) and creep rupture, low-cycle and high-cycle thermo-mechanical fatigue, fracture and a number of additional modes of failure including chemical reactions with the combustion gases [Refs.13- 20].

Fretting fatigue failure can occur in the blade-disk attachment at the fir tree joint, as shown in Fig.4 [Ref.17]. This joint is nominally fixed but micro scale relative movement at the interface occurs between the root and the disk due to the centrifugal forces and tangential vibrations. This combination can cause damage and fatigue failure [Ref.21, 22]. Blade-root attachments are shot peened to induce residual compressive stresses, which are good against fatigue.

The combustion products can include hydrogen, oxygen, CO, CO_2, sulfur, NaCl (when the plane flies over the ocean), solid carbon particles, etc. At the high temperatures, many of these chemical species can contribute to hot corrosion of the turbine blades [Refs.17, 23].

High temperature oxidation [Ref.16] occurs when nickel-based super alloy blades are exposed to high temperatures. The oxygen in the combustion gases reacts with the nickel to form a nickel oxide layer on the blade surface. The nickel oxide layer cracks and spalls due to vibration and thermal cycle starts and stops. This process can occur on the inside surfaces of blade cooling passages also. To prevent such blade failure modes, coatings are applied on the blade exterior and cooling passage interiors.

Sulphidation is a chemical reaction that occurs when sulphur compounds such as SO, SO_2 and SO_3 from the ingested air or combustion products combine with NaCl; sea, industrial and agricultural salts present in the air enter aircraft gas turbines and sulphur is a common impurity in almost all liquid petroleum fuels. The chemical reactions between the sulphur compounds and sodium chloride result in droplets of sodium sulphate (Na_2SO_4) which is highly corrosive. It can attack the protective ceramic coating and then the super alloy substrate. Deep stress raiser pits can form on the blade and lead to other forms of damage and failure [Refs.16, 24, 25]. A summary of the early corrosion observed in aircraft engines is found in a NATO Report [Ref.26]. Many reviews of sulphidation corrosion have been published [Refs.27-29].

Cracking can initiate near the root of the blade (where the centrifugal stresses are high) by a mechanism of Low Cycle Fatigue (LCF) induced during thermal loading cycles. Such a cracked blade is shown in Fig.5 [Ref.30]. Here the crack propagation was aided by environmental attack.

One of the two innovations to increase the turbine inlet temperature while minimizing the detrimental effects on the blade alloy consists of circulating cooling air through passages and holes in the blade. These holes are susceptible to damage due to a variety of causes. A first stage gas turbine blade with the cross section showing a number of cooling holes is shown in Fig.6 [Ref.31]. Three sections at 10%, 60% and 90% heights are indicated. Cracks at holes at the 60% and 90% heights were observed as the temperature was high towards the blade tip. Cracking at the cooling holes was due to grain-boundary oxidation and nitridation at the cooling hole surface, embrittlement (loss of ductility) of the super alloy. The temperature gradient from the airfoil surface to the cooling holes resulted in high thermal stresses at the holes located at the thicker sections of the blade. The cooling hole contributed a stress concentration factor of 2.5 and a relatively high total strain at the cooling hole surface. The oxidation and cracking at one of the holes, after 32,000 hours of operation, is shown in Fig.7(a) [Ref.31]. A crack found on the surface of No.5

cooling hole due to oxidation is shown in Fig.7(b). The surface of the hole was not coated.

It has been found [Ref.32] that most of the failures in aero engine turbine blades are due to microstructural changes at elevated temperatures, hot corrosion and degradation of mechanical Properties resulting in creep and failure due to creep-fatigue interaction.

A very important question to answer in aircraft maintenance is: what is the time interval between inspections or overhauls or refurbishments? When a new engine is designed and placed in service, it is brought in early for overhaul [Ref.13] after 10,000 hours. When experience and confidence are gained with an engine type, the first overhaul is after 22,000 hours. The second overhaul is done after 15,000 hours. Turbine blades removed from service are repaired or refurbished two or more times. If the thermal barrier coating is damaged, the blades are completely stripped of their coatings and recoated. New abrasive tips are installed and the blade roots are shot peened.

The engine is borescoped periodically to detect damage. A high pressure turbine blade that has not suffered appreciable damage and one that has suffered oxidation, spalling and thermo-mechanical fatigue cracks are shown in Fig.8 [Ref.13].

Other forms of damage to the turbine blades are erosion due to solid particles (such as carbon, silica, etc.), erosive wear and Foreign Object Damage (FOD). Apart from particulate erosion, there also exists the important hot gas erosion.

Turbine Blade Materials

Increasing air traffic, rising fuel prices (with the exception of occasional dips) and environmental concerns have all combined to increase the demand for gas turbine engines with higher fuel efficiencies. The thermal efficiency of an engine depends directly on the Turbine Inlet Temperature (TIT). In the last 60 years this temperature has risen from about 600°C to more than 1500°C, causing the engine thrust to increase by 60% and fuel consumption to decrease by 20%. This increase in the TIT has been mainly due to three factors: (i) advances in the blade materials, (ii) the innovative design and fabrication of blade cooling passages, and (iii) the innovative thermal barrier coatings on the blades. The blade cooling and the thermal barrier coating allow the blade to operate at about 300°C above the melting point of the blade alloy. Only about 30% of the increase in turbine inlet temperatures is due to improvements in turbine blade alloys. The rest of the 70% increase in TIT is due to the blade cooling technology and the ceramic coating applied to the metallic blade [Ref.4].

The early jet engines by von Ohain and Whittle utilized nickel steels or stainless steels [Refs.33, 34]. They had a temperature limitation of about 450° to 500°C as their strength decreased rapidly beyond this range [Refs.35, 36].

The variation of specific strength (tensile strength divided by specific gravity) of some common alloys with temperature is shown in Fig.9 [Ref. 37]. Aluminum alloys have a relatively low specific gravity of 2.7 but their strength is relatively low and they are susceptible to overaging at relatively low temperatures. Therefore, the specific strength of aluminum alloys falls rapidly as the temperature increases. Steels are strong but their specific gravity is high, around 7.8. Therefore their specific strength is low and as mentioned earlier, the strength of steel drops drastically around 500°C. Titanium alloys have a relatively low specific gravity of 4.5 and good strength at low temperatures. Thus their specific strength is high at low temperatures but it drops rapidly around 450°C. The figure shows that the nickel alloys, termed super alloys, retain their strength at temperatures of the order of 1000°C. The specific gravity of nickel is 8.9 but having a Face-Centered-Cubic (FCC) crystal structure, nickel and nickel-based alloys (super alloys) are less sensitive to temperature variations.

Whenever a new material or process is to be implemented in the aerospace industry, in addition to the usual steps such as concept definition, and product realization the product or process has to meet stringent certification requirements. Only then can the product (turbine blade) be produced, delivered to the customer and customer support provided. The whole process can take approximately ten years.

Shortly after the stainless steel blades were made for the Whittle engine and the Ohain engine, nickel-based alloys were developed. These alloys were called "super alloys" because they were superior to the earlier steels and the cartoon character, "superman", had just been created in 1938. Super alloys exhibited outstanding tensile strength, creep strength and fatigue strength at high temperatures (continuously raised by changes in alloy chem-

istry), excellent ductility and toughness. During the 1950s, several families of heat resistant alloys were made: "Nimonic" series in England, "Tinidur" alloys in Germany and "Inconel" alloys in USA [Ref.34].

Nickel-based super alloys were made in the 1940s and were steadily improved in the subsequent decades for gas turbine blades. Super alloys have been called "reigning aristocrats of the metallurgical world" [Ref.38]. Cobalt-based super alloys underwent a less dramatic evolution [Ref.39] and have been preferred for vanes and other non-rotating high temperature components due to their good castability, resistance to thermal fatigue, hot corrosion and oxidation and repairability. The first nickel-based super alloy for turbine blades was Nimonic 75, made in the 1940s. In 1951-52, it was confirmed that the strengthening in super alloys was due to the age-hardening of the coherent precipitate γ' (Ni_3Al, Ni_3T_i) in a nickel rich matrix γ [Ref.39]. In 1957 the surprising discovery was made that γ' becomes stronger with increasing temperature over the temperature range of 600° to 800°C- instead of suffering the usual "Oswald ripening effect" [Ref.40].

Along with the changes in the chemistry of the super alloys, another development responsible for the outstanding properties of super alloys was the introduction of vacuum induction melting around 1950. This development had the dual advantages of eliminating detrimental trace and minor elements and allowing the addition of reactive elements in the melt.

The progress in the super alloy chemistry through the 1960s, 1970s, 1980s and 1990s was often "chaotic and undisciplined" [Ref.34] as "much work was done in secret, propriety fashion". Modern nickel-based super alloys can contain ten or more alloying elements , each added for specific reasons (Table-1).The chemistry of super alloys is partly logic and partly (or mostly) magic; it is an art, similar to cooking. Additions of refractory elements like Re, W, Mo, etc., have led to the development of multiple generations of super alloys [Ref.41-50]. These refractory elements provide high degrees of solid solution strengthening. But these elements also promote the formation of Topologically Close Packed (TCP) phases, which are detrimental to mechanical properties at elevated temperatures; further, the oxidation resistance is also compromised due to elements like Mo, Re, Ru, etc. There are other disadvantages of refractory metal additions such as increase in cost and density and decrease in castability and microstructural stability.

Nickel-based super alloys derive some strength from solid solution strengthening but precipitation hardening imparts more significant high temperature strength. The major phases present in most nickel-based super alloys are [Ref.51]: (i) Gamma (γ), which is the FCC Ni-based austenite phase matrix that usually contains a high percentage of solid- solution forming elements such as Co, Cr, Mo and W. (ii) Gamma prime (γ'), which is a coherent precipitate and the primary strengthening phase. It is chemically compatible with the matrix and exceptionally stable over long time. While it is strong, it is also quite ductile. (iii) Carbides such as TiC, TaC, HfC, etc., which are formed by carbon which is usually present at levels of 0.05% to 0.2%, in combination with reactive refractory elements such as Ti, Ta, Hf, etc. During heat treatment and high temperature service, these carbides begin to decompose and form other carbides on the grain boundaries; in general, these carbides forming on the grain boundaries are beneficial. (iv) TCP phases, which are generally brittle and form during heat treatment or during high temperature service. The microstructure of TCP has close-packed atoms in layers separated by relatively large interatomic distances, resulting in a characteristic "topology". In contrast, γ' is close-packed in all directions and is termed Geometrically Close Packed (GCP). TCPs tie up γ- and γ'-strengthening elements in a non-useful form, thus reducing creep properties; in addition, being brittle, they can also become crack initiators.

Directionally Solidified (DS) Super Alloys

'Equicohesive Temperature' (ECT) of an alloy is that temperature at which the grain-interior and the grain-boundary are equally strong. Below this temperature, the grain boundaries block dislocation movement and thus enhance the strength of the alloy; therefore a fine-grained material is beneficial (for strength). Above ECT, the grain boundaries become regions of weakness due to grain boundary sliding, facilitating creep; therefore a coarse-grained material is beneficial.

The major loading on a gas turbine blade produces centrifugal stresses; the advantage of producing columnar grains aligned with the blade axis consists of producing a grain structure that has a minimum amount of grain boundaries perpendicular to the centrifugal stress direction. The process used for producing this columnar grain structure, instead of the equi-axed or randomly oriented grain structure, was "Directional Solidification" (DS). For the same chemical composition, a super alloy blade made by DS had superior high temperature resistance compared

to a conventionally solidified super alloy blade having equi-axed grains.

The DS process has been used to produce both oriented columnar-grained as well as Single Crystal (SC) turbine blades. The DS process is illustrated in Fig.10 [Ref.52]. A group of blades, called a "cluster" and consisting of 10 to 30 blades, are oriented in a circular pattern for thermal uniformity. A thin-walled ceramic mold is created by lost wax process for investment casting (described a little later). It has a pouring basin and runner to each blade cavity in the cluster. The mold is placed in an induction furnace and molten super alloy is poured into the pouring basin. There is a chilled copper plate at the bottom at which solidification begins. The mold is withdrawn downwards. Blades with columnar grains aligned with the direction of withdrawal of the mold are produced. The same DS process is also used to produce SC blades by incorporating a grain selector which is spiral shaped or pig-tail shaped, as shown in Fig.11 [Ref.53]. The turbine blades with equiaxed grains, directionally solidified columnar grains and directionally solidified single crystal are shown in Fig.12 [Ref. 37].

The grain selector that allows one grain to grow into a blade is shown in Fig.13 [Ref.54]. The molten metal in contact with the chill plate (at the bottom) solidifies first and columnar grains start to grow parallel to the direction of mold withdrawal. After the columnar grain starter block, a single grain continues to grow through the spiral or pig-tail grain selector. The spiral is followed by the actual blade form where the melt continues to solidify into one grain or crystal. The preferred crystallographic orientation is < 001 > which is the direction with the lowest Young's modulus. When a constant strain (creep) is considered, the stresses will be lower for this direction and therefore the thermal fatigue life will be enhanced. The steady increase in the turbine blade temperature over the years due to the improvements in the blade materials and blade manufacture is shown in Fig.14 [Refs.55, 56].

The three main advantages of single crystal blades over the conventionally cast (equiaxed grains) and DS (columnar grains) blades are [Ref.55]: (i) Elimination of grain boundaries transverse to the principal tensile stress axis reduces grain boundary cavitations and cracking, resulting in greatly enhanced creep ductility. (ii) Elimination of grain boundary strengthening elements, such as carbon, boron, and hafnium which become redundant (Table-1), [Ref.45]. This has facilitated heat treatment and allowed for further optimization of the alloy chemistry to increase the high temperature capability. (iii) The preferred < 001 > crystallographic solidification direction minimizes the thermal stresses developed on engine- startup and shut-down. This has dramatically enhanced the thermal fatigue resistance of the turbine blade.

Table-1 : Alloying Elements in Super Alloys and their Beneficial Effects [Based on Refs. 44, 45]

Benefit	Alloying Elements
Solid solution strengthening	Co, Cr, Fe, Mo, W, Ta, Re
Grain boundary strengthening	W, Ta, Ti, Mo, Nb, Hf, Cr
g' precipitate formers	Al, Ti
Oxidation resistance	Al, Cr, Y, La, Ce
Hot corrosion resistance	Cr, Co, Si, La, Th
Grain boundary refinement	B, C, Zr, Hf

While blades with < 001 > orientation have higher temperature creep strength compared to other orientations, it is not unusual to have deviations from this preferred orientation. In general, blades with less than 10° deviation from the preferred orientation are judged to be well oriented [Refs.56, 57].

Evolution of Single Crystal Super Alloys

The SC super alloys have evolved over the years, as shown in Table-2 [Ref.44]. The first real improvement in the SC super alloy chemistry was the introduction of Rhenium. This refractory element improves the creep properties appreciably due to solid solution strengthening; more importantly, Re slows all thermally activated high temperature deformation and damage mechanisms due to its low diffusion rate. While the first generation SC super alloys had no Rhenium (Re: melting point = 3185°C, specific gravity = 20.8) or Ruthenium (Ru: melting point = 2334°C, specific gravity = 12.45), the second and third generations of SC super alloys had approximately 3% and 6% Re respectively and no Ru. Typical second generation SC super alloys are Rene N5, CMSX-4 and PWA 1484, widely used for turbine blades in aircraft engines and land-based gas turbine engines. Rene N6 and CMSX-10 are examples of third generation SC super alloys. The drawbacks of adding Re, outweighing the benefits were high cost, susceptibility to casting defects, increase in density and the formation of TCP precipitates. Another

Table-2 : The Evolution of Single Crystal Super Alloys (Based on Refs. 44, 45]

Generation	Re and Ru Content	Typical Alloys
First	No Re or Ru	Rene N4, PWA 1480
Second	~3% Re and no Ru	Rene N5, PWA 1484
Third	~6% Re and no Ru	Rene N6, CMSX 10
Fourth	~6% Re and ~3% Ru	EPM 102, TMS 138
Fifth	~6% Re and ~6% Ru	TMS 162, TMS 196
Sixth	~6% Re and ~6% Ru (but other refractory elements reduced)	TMS 238

problem was the reduction in high temperature oxidation resistance. The precipitation of TCP phases can be suppressed by adding Ru. The Ruthenium improves the stability of the microstructure [Ref.42], increasing the high temperature creep strength, however, the oxidation resistance tends to suffer. In the fourth, fifth and sixth generation SC super alloys, Re was kept around 6% and Ru was increased from 3% (4^{th} generation) to around 6% (5^{th} and 6^{th}). It was found [Ref.42] that additions of Ta, Hf and Y improve the oxidation resistance in 4^{th} generation SC super alloys. In the fifth generation SC super alloys, as shown in Table-2, Ru was increased to about 6% to improve the phase stability [Ref.44]. TMS-196, for instance, contains higher Ru, Re and Cr over the 4^{th} generation alloys. The Cr provides acceptable oxidation resistance.

Utilizing the chemistry of the fifth generation SC alloy TMS-196 as the base, the composition has been tweaked [Ref.43] to develop the sixth generation alloys that exhibit high temperature creep strength and oxidation resistance: Co, Al and Ta have been increased in TMS-238 compared to TMS-196, while Mo and W have been decreased.

Mechanically Alloyed (MA) Super Alloys

Dispersion strengthened super alloys are metal matrix alloys in which a very small volume fraction (1 to 2%) of very fine (micron or submicron size) dispersoids (ceramics or intermetallic compounds) are uniformly dispersed. The dispersoids impede the movement of dislocations and thus impart strength, especially high temperature creep strength, to the super alloys. Among the various ceramic powders, oxides such as Yttria and alumina are very effective. Among the remarkable characteristics of such composites is the retention of high strength at high temperatures- to a very high fraction of the absolute melting point of the matrix alloy [Refs.58-60].

"Mechanical Alloying" is a very useful method to prepare dispersion strengthened composites. Here, the matrix metal and the dispersoid material are introduced in a dry ball mill. When these materials are tumbled with large spheres of a hard material, the constituent materials of the MA alloy are repeatedly welded together and fractured. The blended material is later processed by a metal forming process into a turbine blade. "ODS" alloys refer to oxide (such as Yttria) dispersion strengthened super alloys. The dispersion strengthening is retained at the high service temperatures long after the precipitation hardening (due to the γ' precipitate) disappears. In addition, dispersion strengthened super alloy blades do not need internal cooling passages; thus the expense of making the cooling passages as well as the aerodynamic inefficiencies due to the cooling air can be avoided. But MA super alloy blades have not become popular due to various reasons, including cost. Inconel MA 754, Inconel MA 6000, Alloy 51, etc., are examples of dispersion strengthened alloys.

Directionally Solidified Eutectic Super Alloys

Here, the matrix and the reinforcing phase, in the form of single crystal whiskers, are formed simultaneously during the directional solidification [Ref.61]. In these alloys the matrix is a Ni-based or Co-based super alloy. The reinforcement can be tantalum carbide or vanadium carbide whiskers which solidify aligned with the direction of withdrawal of the mold from the furnace, which is also the length direction of the turbine blade. TaC has a very high melting point (3880°C) and an elastic modulus twice that of steel (400 GPa). The interfacial bond strength between the whiskers and the matrix is excellent. Ni-TaC and Co-TaC have promise. The disadvantage of these materials, also known as in situ composites, is that the volume fraction of the whisker reinforcement is limited to the eutectic composition. Another eutectic that has promise for turbine blade materials is a Ni- or Co- based alloy reinforced by Ni_3Nb lamellae.

A Co-Cr-Ni matrix, reinforced by TaC in a directionally solidified eutectic alloy, has been investigated for its thermal fatigue properties [Ref.62]. While such eutectic

super alloys appear to have some potential for high temperature applications, they have not become popular for gas turbine blade applications- perhaps because of the limitation on the volume fraction of the whisker reinforcement phase, mentioned earlier.

Turbine Blade Fabrication

The manufacturing process for the gas turbine blade has evolved over the years. When the gas turbine blade design was simple, forging could be done. With the increasing complexity of the blade geometry, especially incorporating cooling channels, casting was necessary. As casting introduced porosity, HIPping (Hot Isostatic Pressing) became necessary to reduce porosity. As the blade roots experience very high centrifugal stresses, they were shot-peened to introduce residual compressive stresses which enhanced fatigue life.

In the 1950s, "investment casting", also called "lost wax process", was introduced for blade manufacture. This method had the twin benefits of (i) facilitating directional solidification to produce oriented grains as well as single crystal blades and (ii) using ceramic cores to produce internal cooling channels.

Investment casting is a very old manufacturing process applicable to a wide variety of alloys, especially those with high melting temperatures. Parts with complex geometry can be made by this method. Vacuum melting of super alloys for pouring into the ceramic molds reduced contamination. Investment casting was initially used for producing super alloys with equi-axed (randomly oriented) grains; later, blades with elongated grains and blades with single crystals were made.

The major steps in the investment casting process are the following [Refs.55, 63-65]:

- Pattern creation by injecting molten wax into a metal mold. Ceramic cores are positioned for relatively large cooling passages.
- A number of wax patterns are connected together with a common gating system so that molten metal can be poured into several molds.
- The pattern tree is invested (dipped) into a ceramic powder slurry repeatedly until the ceramic coating is sufficiently thick.
- The wax is melted by heating.
- Further heating to glaze the ceramic mold.
- Molten metal is poured in the ceramic mold.
- The metal is allowed to cool and the ceramic mold shells are broken.
- Finishing operations are performed on the blades.

The major steps involved in investment casting are shown in Fig.15 [Ref.66]. The ceramic cores are positioned using pinning wires [Ref.65]. The pinning wires should be able to function at very high temperatures - up to the melting point of the super alloy. The pinning wire should eventually dissolve and disperse within the super alloy without poisoning the precipitation hardening reactions within the super alloy. Oxide dispersion strengthened platinum (melting point of platinum = 1768°C) has been considered for the pinning wire application [Ref.65]. Palladium (melting point = 1555°C) is also a candidate for this application as it has comparable oxidation resistance, lower specific gravity (11.9 for palladium vs. 21.45 for platinum) and lower cost. To improve the high temperature resistance, refractory metals such as molybdenum, tungsten and platinum are added to palladium.

Turbine Blade Cooling

In this section, the need for blade cooling, different cooling techniques and the methods of machining the cooling channels are discussed [Refs.67-77].

The high pressure turbine blade operates at about 1500- 1600°C and as explained earlier, there is a constant push to raise the TIT (Turbine Inlet Temperature) to higher values. It was earlier mentioned that changes in super alloy chemistry, DS (Directional Solidification), SC (Single Crystal) solidification, etc., as well as innovative changes such as blade cooling and TBC (Thermal Barrier Coating) have responded to the challenge and have made dramatic increases in TIT possible. However the quest for even higher temperatures continues.

The air to cool the blades is drawn from the HP (High Pressure) compressor, routed through the engine core to the blade root; the temperature of this air is around 650°C [Refs.78, 79] and the pressure is high enough so that it can be forced through the intricate cooling channels. By internal and external cooling, the cooling air keeps the blade temperature down to about 1150°C [Refs.78,79]. There are two disadvantages to this kind of blade cooling: first, the air drawn from the compressor (up to 20 per cent of

the compressed air) is not available for combustion of the fuel; second, when the cooling air exits from the blade, it mixes with the main stream of combustion gases, introducing aerodynamic inefficiencies.

Among the many types of cooling, the three predominant ones are: convection cooling, impingement cooling and film cooling. The passages along the length of the blade, created by positioning ceramic cores during investment casting as mentioned earlier, are shown in Fig.16 [Ref.80]. The compressed air, driven by the pressure differences and the centrifugal forces, travels from the blade root to the blade tip, and carries some of the heat acquired by the blade from the combustion gases. In order to improve this heat transfer, a "serpentine" multi-pass path for the cooling air is provided as shown in Fig.17 [Ref.81]. In this figure, the radial cooling passages provide a quintuple- pass pathway so that there is greater heat transfer.

In addition, to make the cooling air linger within the blade longer and thus remove more heat, the passages are "turbulated" by providing ribs, pins and even dimples on the inside surfaces of the blades. The ribs and pins and other strategies are shown in Fig.18 [Ref. 67]. All these devices increase secondary flows and turbulence levels to increase mixing and vortices; they also increase the surface area for increased heat transfer. The goal of the internal blade cooling is adequate thermal protection of the blade with minimum coolant air.

The leading edge of the blade is characterized [Ref.76] by a small coolant metal area to hot gas metal area ratio. The thin trailing edge poses geometric constraints on passage sizes and cooling air accessibility. Rib turbulators are long bars with a rectangular cross-section fixed at an angle to the airflow direction. They protrude into the flow, causing flow mixing and vortices. The dimensions of these turbulators can be optimized to cause the desired heat transfer. Pin-fin arrays are arranged in arrays [Ref.76] and extend between opposite walls of an internal cooling passage. Trailing edges of blade airfoils are candidates for pin-fin arrays as higher levels of heat transfer are required. One of the difficulties of extracting heat from the blade in the trailing edge is that the coolant has already acquired considerable heat by the time the cooling air reaches this region.

While the "dimpled" surfaces (indentations or undulations) on the inside surfaces are usually hemispherical, other shapes have been used. They aid heat transfer by causing multiple vortex pairs. By not protruding into the flow, dimples cause low pressure drops. Thus air bled from low pressure stages of the compressor can be used.

The simplest and the first method of blade cooling is convection cooling [Ref.82]. In this method, the cooling air is made to flow from the blade root to the blade end through the internal passages within the blade. The number and size of the internal passages within the blade as well as the quantity of cooling air available determine the effectiveness of convection cooling.

The second type of cooling is "impingement" cooling, shown in Fig.19 [Ref. 83]. This type of cooling is commonly used near the leading edge of the turbine blade where the heat load is maximum. An insert with tiny holes perpendicular to the blade length is placed in this region inside the blade. Instead of the cooling air traveling quickly along the length of the blade, the air is made to impinge normal to the blade inside surface and thus more heat is dissipated.

The third type of cooling is "film cooling". As shown in Fig.20 [Ref.84], the cooling air that travels from the blade root to the blade tip enters the suction side and the pressure side along the length of the blade through tiny holes. The cooling air is injected into the boundary layer of the hot combustion gases. Thus the blade surface is surrounded by a film of cool air that prevents the blade material from reaching the temperature of the combustion gases. This type of cooling is more effective than convection cooling or impingement cooling. The air used for film cooling must be under high pressure as it is dissipated quickly by mainstream hot gases.

A comparison of the effectiveness of the three cooling methods is given in Fig.21 [Ref.82]. The figure shows that the contribution of the film cooling to the TIT (Turbine Inlet Temperature) is the greatest. The increase in TIT over the years due to the combined effect of the different types of cooling is shown in Fig.22 [Refs.84, 85].

The design and optimization of cooling channels in a turbine blade have been the subject of research for many years by many researchers. The temperature distribution for a blade without cooling channels and the temperature distribution for a blade with cooling channels, obtained by analysis, are shown in Fig.23 [Ref.72] and Fig.24 [Ref.73], respectively. It is seen in Fig.23 that when there is no cooling, most of the turbine blade is at the maximum temperature whereas much of the blade surface is at cooler temperatures (Fig.24) when there is blade cooling.

Turbine blade tip cooling is also important because turbine blade tip leakage flow from the blade pressure side to the suction side over the tip surface increases the thermal load at the blade tip [Ref.86], increasing the local temperature. Leakage flow can be reduced by employing a recessed or squealer tip blade or by cooling the blade tip by incorporating film cooling holes.

Machining Cooling Holes in the Gas Turbine Blades

As explained earlier, the relatively large cooling passages in the turbine blades are incorporated in the blades during investment casting by positioning ceramic cores. Many other passages are smaller, especially the film cooling holes. These require special equipment and techniques. The commonly used techniques for creating the cooling holes are:

- Water Jet drilling (WJ)
- Abrasive Water Jet drilling (AWJ)
- Electro Chemical Machining (ECM)
- Electric Discharge Machining (EDM)
- Electro Chemical Discharge Machining (ECDM)
- Electron Beam Machining (EB)
- Laser Drilling
  - Single Pulse
  - Percussion
  - Trepanning
  - Microjet

The blades are eventually coated with a thermal barrier coating. One of the major decisions to be made at the beginning is whether the cooling holes should be machined in coated or uncoated blades; in other words, should it be coat and drill or drill and coat? If the blade is coated first (with a ceramic coating), then methods that need an electrically conducting blade cannot be used. If the coating is applied after drilling, the coating may clog or partially close the holes, especially the very small ones.

In WJ drilling, water is forced through a tiny orifice at speeds of up to three times the speed of sound. In AWJ, an abrasive powder such as silica or garnet is added to the water [Refs.87-89].

Electro Chemical Machining (ECM) is a machining process in a metal that involves the removal of material by electrochemical corrosion. A high current is passed from a positively charged workpiece through an electrolyte solution to the negatively charged cutting tool [Ref.90]. A shaped electrode is used to create turbulated cooling holes.

Electric discharge machining (EDM) is a thermal process that uses spark discharges to erode material from the workpiece. A rapid series of electrical discharges pass between the electrode and the workpiece (the turbine blade). A dielectric fluid continuously flows and flushes away the chips or debris from the machining process. Intricate cavities, contours and holes can be machined in electrically conducting (uncoated) workpieces (turbine blades).

Electro chemical discharge machining (ECDM) is a hybrid process [Ref.91] combining the principles of EDM and ECM. It is mainly used for micro-machining hard, brittle, non-conductive (coated) materials (turbine blades). Here the tool must be continuously dipped in an electrolyte.

Electron beam machining (EBM) is good for machining holes with consistent accuracy and at a rapid rate. In this method, highly accelerated electrons are focused [Ref.92] on the workpiece surface. At the impact spot, the kinetic energy from the electrons melts and vaporizes the workpiece material. The process is conducted in vacuum. Complex contours can easily be machined by maneuvering the electron beam using magnetic deflection coils.

The main advantage of laser drilling is that it is a non-contact technique and therefore coated blades can also be processed. High aspect ratio holes can be drilled. High speeds and good accuracies are achievable. Like the electron beam machining, there is a process zone consisting of heat affected region, melted material and vaporized zone.

Laser drilling has several variations, such as single pulse, percussion, trepanning, Microjet, etc. In percussion drilling, several laser pulses are used in rapid succession. Trepanning is the technique where first a small hole is drilled and is then enlarged by the laser beam. Laser ablation can remove the thermal barrier coating (TBC) and the bond coat before drilling the holes. Assist gas (process gas) can be used with the laser beam to remove the debris from the cutting area; the gas also cools the workpiece.

During any machining process, using a coolant serves many purposes: it cools the cutting zone, lubricates the process and washes away the debris. In laser Microjet

machining [Ref.94, 95], the laser emitter is surrounded by a water jet and the laser beam travels along the inside of the very narrow stream of water (Fig.25), [Ref.93].The laser beam is contained within the water jet and reflects along the air-water interface. The concentrated laser beam and the narrow water jet hit the workpiece together. The water jet acts as an optical fiber, guiding the laser beam into the workpiece (turbine blade), while cooling the surrounding area and flushing out the drilling debris. It took the GE three years and 1.7 million euros to perfect the laser microjet technology for the gas turbine industry [Ref. 94].

Thermal Barrier Coatings (TBCs)

In this section, the following topics are discussed: why are coatings needed? What is a TBC? What are the materials for the coatings? How are coatings applied on the blades? And how can the coatings fail?

As mentioned earlier, there is a constant push to raise the Turbine Inlet Temperature (TIT) in order to improve the thermal efficiency of aircraft jet engines. Improvements in blade materials (super alloys at present) have almost reached a saturation point. Significant improvements have been achieved with blade cooling. Further improvements are possible only with Thermal Barrier Coatings (TBC) applied to the super alloy blades. As shown in Fig.26 [Ref.95] the increase in TIT due to the improvements in super alloy chemistry and single crystal solidification has been modest compared to the gains achieved by blade cooling and TBC. Originally introduced to stationary engine parts, in the late 1980s TBCs were used on rotating blades. About 1 to 1.5 million kilograms of Yttria Stabilized Zirconia (YSZ) topcoat was Atmospheric Plasma Sprayed (APS) onto engine components in 2011 alone [Ref.96]. Another point to note here is that in the development of the super alloy blade chemistry, the improvements in mechanical properties have been achieved at the expense of resistance to oxidation and corrosion; the TBC compensates for this situation.

The Thermal Barrier Coating (TBC) consists of three layers: (a) a "bond coat" applied directly on the super alloy blade, (b) a ceramic "top coat" applied as an overcoat, and (c) an intermediate "Thermally Grown Oxide" (TGO) layer that develops between the bond coat and the top coat; it is mostly α-Al_2O_3.

The three-layered TBC is shown in Fig.27 [Ref.97]. The figure shows the bond coat which is about 100 μm thick, the top coat which is 100 to 400 μm thick and the TGO that develops between the bond coat and the top coat, 1 to 10 μm thick. The temperature gradient across the coated blade is also shown. The temperature drops across the cooling air film, across the top coat, across the bond coat and finally across the internally cooled super alloy blade.

TBCs are multi-functional. They must provide thermal insulation. They must have strain compliance to minimize thermal expansion mismatch stresses; they (the top coat part of TBC) must be porous (about 15%) for high strain compliance and reduced thermal conductivity. They must reflect radiant heat from the hot combustion gases impinging on the blades. They must withstand extreme thermal gradients (of the order of 1°C/μm) and energy fluxes. They must operate in an oxidizing environment at pressures of 10 atmospheres and gas velocities exceeding Mach 1. In addition to all these requirements, they must also withstand corrosion, erosion, Foreign Object Damage (FOD), etc.

The materials selected for the top coat and the bond coat are different. The top coat, among other things, must have a very low thermal conductivity. The most widely used material is 7YSZ, ZrO_2 stabilized with 7 weight percent Y_2O_3. YSZ has one of the lowest thermal conductivities at elevated temperatures, of all ceramics. YSZ also has a high thermal expansion coefficient, which helps alleviate stresses arising from the thermal expansion mismatch between the ceramic top coat and the super alloy substrate. To further alleviate these stresses, microstructural features such as cracks and porosity are deliberately introduced into the top coat, rendering it highly compliant and strain tolerant. While the top coat porosity is good for strain compliance, it allows easy ingress of oxygen from the combustion gases to the bond coat; even if the top coat were fully dense, the extremely high ionic diffusivity of oxygen in the zirconia-based ceramic top coat renders it "oxygen transparent" [Ref.97]. YSZ has a relatively low specific gravity of 6.4 which is important for rotating engine components. It has a hardness close to 14 GPa, which makes it resistant to erosion and FOD. YSZ is resistant to ambient and hot corrosion. It has a high melting point (close to 2700°C).

New top coat materials being investigated are: pyrochlor materials based on the fluorite structure of zirconia, Perovskite-structured oxides and lanthanide orthophosphates and silicates [Ref.98].

The bond coat in many ways has to meet the most stringent constraints [Ref.95]. One of its primary functions is to provide a reservoir from which aluminum can diffuse outward to combine with the oxygen, diffusing inward through the porous top coat, to form α-Al_2O_3 in the TGO layer. The bond coat has to maintain cohesion with the TBC without reacting with it. There is a constant effort to improve bond coat materials. For instance, adding 1 to 2% Re (melting point = 3180°C, specific gravity = 21) to MCrAlY (M =Co or Ni) coatings makes the coating have better oxidation resistance and better mechanical properties; it also prevents the aluminum from diffusing back into the super alloy substrate.

Ideally, the Thermally Grown Oxide (TGO) should remain elastic at the highest temperatures encountered without creep, which can cause "rumpling", or cavitation; during thermal cycling creep can cause the development of local separations at the TBC interface. At the same time, the TGO has to operate at the highest possible temperature so that the amount of cooling air needed can be minimized.

There are various methods for depositing ceramic coatings on metal (super alloys) substrates. Out of these the two most important methods used for TBC top coat deposition are (a) Air-Plasma-Spray (APS) deposition and (b) Electron Beam Physical Vapor (EB-PVD) deposition. Both these methods, on the whole, produce the desirable microstructures and characteristics. In APS, μm sized particles of metals and ceramics are introduced in powder form into an arc-plasma jet and projected onto a prepared substrate. The particles melt, followed by impact and rapid solidification. In EB-PVD, a highly energetic electron beam is scanned over the ceramic material to melt and vaporize it within a vacuum chamber. The preheated substrate is positioned in the vapor cloud and the vapor is deposited onto the substrate.

APS TBC provides much less strain resistance than the EB-PVD. EB-PVD provides a columnar microstructure, which contributes to strain compatibility and thermal fatigue life. For jet engine applications, TBC coatings deposited by EB-PVD are said to have [Ref.99] higher lifetime compared to APS; but for land-based turbines, APS is said to give the best performance. The columnar microstructure due to EB-PVD provides pseudo-plasticity. Compared to the APS TBCs, EB-PVD TBCs exhibit a higher erosion resistance, a smoother surface finish that offers aerodynamic advantages, and cooling holes that stay open through the processing. The disadvantages of EB-PVD are high cost, higher thermal conductivity and limits in chemical variability due to vapor pressure issues.

There are several possible failure modes of TBC. The growth of the TGO during the turbo-engine operation is one of the factors responsible for the spallation failure of TBCs. The formation and growth of the α-Al_2O_3 TGO results in the depletion of Al in the bond coat. If this aluminum depletion is severe, other oxides such as Ni- and Co- containing spinals can form. The structural integrity of the TGO is compromised by the formation of these phases and the localized oxidation due to the fast oxygen-diffusion paths accelerates.

Molten deposits can also destroy TBC [Ref.95]. Molten silicate deposits, based on CMAS (Calcium-Magnesium-Alumino-Silicate) can corrode the super alloy blades. CMAS originates from siliceous debris (airborne dust, sand, ash, etc.) ingested with the intake air. At the high temperatures of the combustion gases, the glassy melt can penetrate the porous TBC, chemically dissolve the TBC and cause the precipitation of a modified oxide. The blade is covered by a brownish deposit that strongly adheres to the blade surface. The deposit usually appears on the pressure side and leading edge. The molten CMAS has a low viscosity and infiltrates the inter-columnar gaps in the TBC, pores and cracks all the way to the TGO, as shown in Fig.28 [Ref.100]. Upon cooling, the molten CMAS freezes and the infiltrated TBC becomes rigid and loses its strain compliance. Delamination cracks develop in TBC and lead to spallation during thermal cycling. While solutions to this problem are being explored, one concept is to deposit a thin layer of a non-reactive metal (such as platinum) near the coating surface (Ref. 100) which will arrest the CMAS penetration.

Future Trends

Conventional super alloys (Nickel and Cobalt based), with all the changes in alloy chemistry, cooling passages and thermal barrier coatings, have reached their limit in increasing TIT. Further increases in TIT will have to continue for improving the thermal efficiency of gas turbines, by resorting to other materials. In this section, Iridium based super alloys, intermetallics, bulk ceramics, ceramic composites, directionally solidified eutectic ceramics, transformation toughened ceramics and self-healing ceramics are briefly described.

In the 1960s, refractory alloys based on Nb and Mo were considered for turbine applications; while they are good in inert atmospheres, their oxidation resistance was inadequate. In both Iridium and Platinum based super alloys, the microstructures similar to those of Ni-based super alloys can be obtained [Ref.101]. Iridium based alloys have good creep strength but are marginal in their oxidation resistance. The oxidation resistance of platinum based alloys is adequate but their creep strength is low. More development is needed.

By contrast, Refractory Metal (RM) based metal-intermetallic composites, such as RM-silicides were developed in the 1990s to take advantage of the beneficial oxidation and creep resistance of the silicides and the mechanical properties of the RM. Two of the more promising systems are Mo-based silicides and Nb-based silicides. They form as metal-toughened intermetallic-strengthened materials with a metallic phase volume fraction between 35% and 60% [Ref.102]. The melting points of these multiphase alloys are above 1750°C (Nb-based) and 1950°C (Mo-based), respectively. Mo-Si-B alloys typically have a matrix of Mo solid solution providing fracture toughness and ductility below 600°C and embedded intermetallic Mo_3Si and Mo_5SiB_2 type compounds for creep and oxidation resistance; they exhibit melting points on the order of 2000° C and their room temperature fracture toughness is improved by adding small amounts of Zr [Ref.103]. Alloys of Nb-Si system can be improved by the addition of other elements: for instance, NbTiHfCrAlSi.

Bulk ceramics such as Si3N4 can operate up to 1500°C [Ref.104] and have been used in small land-based turbines. Ceramics offer many advantages over super alloys, such as lower density, better resistance to oxidation and abrasion, etc. But silicon nitride has a few problems such as difficulty in machining due to its hardness, lack of long term reliability and low fracture toughness to withstand FOD. The mechanical properties and machinability of Si_3N_4 can be improved by combining it with $MoSi_2$. When these two materials are combined, there is synergy resulting in increase in fracture toughness and compression strength at room temperature, increase in creep strength at high temperature and decrease in thermal expansion. Further work is in progress in composition optimization, microstructure control, porosity reduction and improvement in the manufacturing process. To increase the high temperature properties of silicon nitride, several additives such as SiC, TiN/TiC, BN, ZrO_2, $MoSi_2$, etc., have been added. These materials can be used at temperatures considerably higher than possible with super alloys.

The push for jet engine fuel efficiency continues with greater vigor. While the average fuel consumption per seat-km today is 27 to 35 per cent less compared to 1980, more ambitious reductions have been called for by the Advisory Council for Aviation Research in Europe (ACARE) in "Flightpath 2050" [Ref.105]. The goals are: a 75% reduction in CO2 per passenger-km, a 90% reduction in nitrous oxide (NOx) emissions and a 65% reduction in noise by the year 2050 compared to 2000. Such drastic reductions require revolutionary materials and ceramic matrix composites (CMCs) offer a solution [Ref.105].

CMCs are considerably more expensive but they are much lighter, stronger and offer a 100 to 200°C improvement in high temperature capability compared to the super alloys. The main types of CMCs include SiC fiber reinforced SiC matrix, carbon/carbon composites, carbon/SiC composite and oxide fiber/oxide matrix composite, where the oxide is typically alumina. SiC/SiC components used in oxidizing environments must be protected using Environmental Barrier Coatings (EBCs). SiC fibers must be coated also to prevent attack from oxygen diffusing through the porous matrix. The oxide fiber/oxide matrix composites do not require a protective coating but they are inferior to SiC/SiC composites in thermo mechanical properties [Ref.105].

A drastic increase in CMCs is expected soon in aeroengine components in the coming years. In addition to their higher temperature capabilities, CMCs, unlike super alloys in the hot zone, do not need to be air-cooled; thus the air flow will be freed to boost the engine's propulsion and efficiency. Although the static components will be made of CMCs initially, eventually greater benefits will accrue when the turbine blades are made of CMCs. CMC rotating parts of military jet engines have already been tested successfully [Ref.105]. Lightweight turbine blades will require lighter turbine disks and bearings multiplying weight savings manifold. In spite of practical problems in material properties and material processing, progress is being made in attempts to bring CMCs to the hot rotating parts of gas turbines [Ref.106-108].

One way to improve ceramics is, just as in the case of super alloys, to directionally solidify them, or their eutectics. Directional solidification of eutectic compositions between alumina and rare-earth oxides result in situ composites of two single crystal eutectic phases. After solidi-

fication, the eutectic phases are alumina and either a Perovskite phase R_EAlO_3 (R_E: Gd or Eu) or a garnet phase $R_{E3}Al_5O_{12}$ (RE: Y, Yb, Er, Dy).

In the case of ternary systems, cubic zirconia is added to improve fracture toughness, as a dispersoid. Both the binary and ternary systems exhibit very good mechanical properties such as flexural strength that is constant up to temperatures close to the melting point, good creep resistance, microstructure stability and oxidation resistance (Ref. 109). For very high temperature structural applications such as turbine blades in future aeronautical turbo engines or land based power units, investigations are in progress in both binary [Al_2O_3-$Y_3Al_5O_{12}$ (YAG), Al_2O_3-$Er_3Al_5O_{12}$ (EAG), and Al_2O_3-$GdAlO_3$ (GAP)] and ternary [Al_2O_3-YAG-ZrO_2, Al_2O_3-EAG-ZrO_2 and Al_2O_3-GAP-ZrO_2] eutectics [Ref.110].

Two novel developments in the field of ceramics can be expected to overcome the traditional drawbacks of ceramics such as brittleness and low fracture toughness and thus make them viable candidate materials for aircraft turbine blade applications. These are crack-healing and transformation toughening.

In crack-healing, when a ceramic develops a crack exposed to the environment, depending on the availability of oxygen, a reaction product of oxygen and one of the constituents of the ceramic can form and seal the crack. For this to happen, the temperature should be high enough and the time should be sufficient. For instance, in a ceramic composite containing SiC, the following chemical reaction can take place [Ref.111]:

$$SiC + 2\ O_2 = SiO_2 + CO_2\ (CO) + 943\ kJ$$

The following three conditions must be satisfied for effective crack-healing: (1) The space between the crack walls must be filled completely with the chemical reaction products, (2) The crack-healing product should be as strong as or stronger than the matrix, and (3) the crack-healing substance must have a strong bonding with the matrix. It has been found [Ref.112] that several ceramic composites show crack-healing characteristics. Examples are: Al_2O_3 + SiC particles, Si_3N_4 + SiC, Al_2O_3 + SiC whiskers, ZrO_2 +SiC, SiC fibers in SiC matrix, etc. Light weight silicon carbide fiber reinforced silicon carbide matrix (SiC/SiC) composite appears poised for applications in the next generation aircraft engines [Ref.112].

As mentioned earlier another novel development in ceramics is transformation toughening. Transformation toughening of ceramics was first reported by Garvie et al in 1975 and the term "ceramic steel" was coined [Ref.113]. Garvie et al showed that the volume increase in the tetragonal to monoclinic transformation in zirconia may be used to increase the fracture toughness of a ceramic through careful control of the composition and microstructure.

High temperature turbine blades fabricated from ceramics (and ceramic composites) need to be coated with a protective coating, very similar to the coating (TBC) applied to super alloy blades. This is because silicon containing ceramics react with oxygen and water vapor at high temperatures and form SiO_2 scales; these then react with the water vapor to form gaseous silicon hydroxide. The protective coating, termed Environmental Barrier Coating (EBC), should impede the diffusion of oxygen and water vapor.

A typical advanced EBC is shown in Fig.29 [Ref.100]. It consists of a silicon bond coat applied directly to a SiC based CMC, a layer of mullite (for impeding diffusion of oxygen to the silicon bond coat) and a low volatilization rate material (such as a rare earth silicate) that protects the mullite and silicon layers from volatilization by water vapor. The EBC can protect the ceramic material/composite at very high temperatures (such as 1700°C). Multilayer EBC systems are usually deposited by thermal spray processes or plasma spray process.

Concluding Remarks

The turbo-engine is a remarkable product of engineering ingenuity in the fields of design, materials and manufacturing and is used in aircraft propulsion as well as land-based power generation. The blades of the high pressure turbine are the most severely stressed components. They are subjected to high centrifugal stresses, high temperatures, corrosion, oxidation, foreign object damage, etc.

There is a constant pressure on the aircraft industry to increase the Turbine Inlet Temperature in order to increase the thermal efficiency of the engine to keep up with the rising fuel costs. Innovations in blade materials have resulted in improvements in the chemistry and microstructure of the nickel-based super alloys. Innovations in the manufacture of the blades have resulted in directional solidification of the blades. Innovations in design have

resulted in internally cooled blades and blades with Thermal Barrier Coatings.

Further increases in the Turbine Inlet Temperatures require the inevitable use of ceramics for turbine blades. The traditional limitations due to brittleness can be overcome by innovations such as ceramic matrix composites with ceramic reinforcements, directionally solidified eutectic composites, transformation toughened ceramics, self-healing ceramics, etc. Ceramic blades also will need an Environmental Barrier Coating. Work is in progress in all the afore- mentioned areas and the actual use of ceramic based materials in the turbo engines, especially the rotating components, is not too far off.

References

1. Ahmad F. El-Sayed., "Aircraft Propulsion and Gas Turbine Engines", CRC Press, 2008, ISBN-13: 9780849391965.

2. Klaus Hunecke., Jet Engines: Fundamentals of Theory, Design and Operation", The Crowood Press, UK, ISBN: 0-7603-0459-9.

3. Airplane Flying Handbook, FAA-H-8083-3A, US Department of Transportation, Federal Aviation Administration, 2004.

4. Owen, J. M., "Developments in Aero Engines", Pertanika Journal of Science and Technology 9(2), 2001, pp.127-138.

5. Torenbee, K. E. and Wittenberg, H., "Flight Physics: Essentials of Aeronautical Disciplines and Technology with Historical Notes", Springer, 2009, ISBN 978-1-4020-8663-2.

6. Golley, J. and Gunston, B., "Genesis of the Jet-Frank Whittle and the Invention of the Jet Engine", Airlife Publishing, Shrewsbury, 1996, ISBN 185310 860 x.

7. Glyn, J., "The Jet Pioneers-The Birth of the Jet-Powered Flight", Methuen, London, 1989, ISBN 0413 50400 x.

8. Gibbs-Smith, C. H., "Aviation: An Historical Survey from its Origins to the End of World War II", London: HMSO, 1970.

9. "Early Gas Turbine History", MIT Gas Turbine Laboratory, http://web.mit.edu/aeroastro/labs/gtl/early_GT_history.html

10. Koff, B. L., "Gas Turbine Technology Evolution-A Designers Perspective", AIAA/ICAS International Air and Space Symposium and Exposition: The Next 100 Y, 14-17 July 20003, Dayton, OH, AIAA 2003.

11. Meher-Homji, C. B., "The Development of the Whittle Turbojet", J. Eng. Gas Turbines and Power, Vol.120, 1998, pp.249-256.

12. Cervenka, M., "The Rolls Royce Trent Engine", 5 October 2000.

13. Zaretsky, E. V., Litt, J. S., Hendricks, R. C., and Soditus, S. M., "Determination of Turbine Blade Life from Engine Field Data", Journal of Propulsion and Power, Vol.28, No.6, November-December 2012, pp.1156-1167.

14. Rao, V. N. B., Kumar, I. N. N., Madhulata, N. and Abhijeet, A., "Mechanical Analysis of First Stage Marine Gas Turbine Blade", Int. Journal of Advanced Science and Technology, Vol.68, 2014, pp.57-64.

15. "Jet Engine Design: The Turbine", Aerodynamics, Manufacturing, Technology, April 6, 2013.

16. Homji, C. B. M. and Gabriles, G., "Gas Turbine Blade Failures- Causes, Avoidance, and Troubleshooting", Proceedings of the 27th Turbomachinery Symposium, Turbomachinery Laboratories, Texas A & M University, Houston, Texas, September 22-24, 1998.

17. Bhagi, L. K., Rastogi, V. and Gupta, P., "A Brief Review on Failure of Turbine Blades", Proceedings of STME-2013, Smart Technologies for Mechanical Engineering, 25-26 October 2013 at Delhi Technological University, Delhi, India.

18. Hou, J., Wicks, B. J. and Antoniou, R. A., "An Investigation of Fatigue Failures of Turbine Blades in a Gas Turbine Engine by Mechanical Analysis", Engineering Failure Analysis, Vol.9, 2002, pp.201-211.

19. Mazur, Z., Rez, L. R. Islas, J. A. J. and Amezcua, A. C., "Failure Analysis of a Gas Turbine Blade Made of Inconel 738 LC Alloy", Engineering Failure Analysis, Vol.12, 2005, pp.474-486.

20. Naeem, M. T., Jazayeri, S. A. and Rezamahdi, N., "Failure Analysis of Gas Turbine Blades", Proceedings, IAJC-IJME International Conference Paper 120, 208, ENG 108.

21. Tang, H., Cao, D., Yao, H., Xie, M. and Duan, R., "Fretting Fatigue Failure of an Aero Engine Turbine Blade", Engineering Failure Analysis, Vol.16, 2009, pp.2004-2008.

22. Rajasekaran, R. and Nowell, D., "Fretting Fatigue in Dovetail Blade Roots: Experiment and Analysis", Journal of Tribology International, Vol.39, 2006, pp.1277-1285.

23. Ebara, R., "Corrosion Fatigue Phenomena Learned from Failure Analysis", Engineering Failure Analysis, Vol.13, 2006, pp.516-525.

24. Boyer, H., E., Editor, "Failure Analysis and Prevention", Metals Handbook, Eighth Edition, 1975, ASM.

25. De Crescente, M. A., "Sulphidation and its Inhibition in Turbomachinery", Proceedings of the Ninth Turbomachinery Symposium, Turbomachinery Laboratory, Texas A&M University, College Station, Texas, 1980, pp.63-68.

26. Stringer, J., "High Temperature Corrosion of Aerospace Alloys", AGARDograph No. 200, NATO Advisory Group for Aerospace Research and Development, Neuilly-sur-Seine, 1975.

27. Bornstein, N., S., "Reviewing Sulphidation Corrosion- Yesterday and Today", JOM, Vol.48, Issue 11, November 1996, pp.37-39.

28. Allen, W. A., and Bornstein, N. S., "Sulphidation Corrosion Revisited", Proceedings of the Fourth International Symposium on High Temperature Corrosion, New York, Elsevier Science Publishers, 1996.

29. Santoro, G. S. et al., "Deposition on Na_2SO_4 from Salt Seeded Combustion Gases of a High Velocity Burner Rig", High Temperature Corrosion of Energy Systems, Edited by Michael Rothman, Warrendale, Pennsylvania, TMS, 1985.

30. Tanzer, A., "Determination and Classification of Damage", Failure Analysis and Prevention, Vol.11, ASM Handbook, ASM International, 2002, pp.343-350.

31. Benac, D. J. and Swaminathan, V. P., "Elevated Temperature Life Assessment for Turbine Components, Piping and Tubing", Failure Analysis and Prevention, Vol.11, ASM Handbook, ASM International, 2002, pp.289-311.

32. Jayakumar, T., Muralidharan, N, G., Raghu, N., Kasiviswanathan, K. V. and Raj, B., "Failure analysis Towards Reliability Performance of Aero Engines", Defence Science Journal, Vol.49, No.4, 1999, pp.311-316.

33. Conner, M., "Hans von Ohain: Elegance in Flight", AIAA, 2001, ISBN: 1-56347-520-0.

34. Schafrik, R., "Materials in Jet Engines: Past, Present and Future", General Manager, Materials and Process Engineering, GE Aircraft Engines, Power Point Presentation.

35. Nathan, S., "Jewel in the Crown: Rolls Royces Single Crystal Turbine Blade Casting Foundry", 8th June 2015, https://www.theengineer.co.uk/jewel-in-the-crown-rolls-royces-single-crystal-turbine-blade.

36. Knight, L., "The Metal that brought you Cheap Flights", Magazine, 16th May 2015, http://www.bbc.com/news/magazine-32749262.

37. Cervenka, M., "The Rolls Royce Trent Engine", Rolls Royce, 5th October, 2000, Power Point Presentation.

38. Cahn, R. W., The Coming of Material Science, March 2001, Pergamon, ISBN: 9780080426792.

39. Taylor, A. and Floyd, R. W., "The Constitution of Nickel-Rich Alloys of the Nickel-Chromium-Aluminum System", Journal of the Institute of Metals, Vol.81, 1952-53, pp.451-464.

40. Westbrook, J. H., "Temperature Dependence of the Hardness of Secondary Phases Common in Turbine Bucket Alloys", Trans. AIME, 1957, pp.898-904.

41. Estrada, ., A. M., "New Technology used in Gas Turbine Blade Materials", Scientia et Technica Ano XIII, No.36, September 2007, Universidad Tecnologica de Pereira, ISSN 0122-1701, pp.297-301.

42. Kawagishi, K., Harada, H., Sato, A. and Kobayashi, T., "The Oxidation Properties of Fourth Generation Single Crystal Based Super Alloys", JOM, January 2006, pp.43-46.

43. Kawagishi, K., Yeh, A. C., Yokokawa, T., Kobayashi, T., Koizumi, Y. and Harada, H., "Development of an Oxidation Resistant High Strength Sixth Generation Single Crystal Super Alloy TMS-238", Super Alloys 2012, 12th International Symposium on Super Alloys, TMS (The Minerals, Metals & Materials) Society, 2012, pp.189-195.

44. Sato, A., Yeh, A. C., Kobayashi, T., Yokokawa, T., Harada, H., Murakuma, T. and Zhang, J. X., "Fifth Generation Nickel Based Single crystal Super Alloy with Superior Elevated Temperature Properties", Energy Materials, Vo.2, No.1, 2007, pp.19-25.

45. Caron, P. and Khan, T., ""Evolution of Nickel Based Super Alloys for Single Crystal Gas Turbine Blade Applications", Aerospace Science and Technology, Vol.3, 1999, pp.513-523.

46. Haselbach, F. and Parker, R., "Hot End Technology for Advanced Low Emission Large Civil Aircraft Engines", 28th International Congress of the Aeronautical Sciences (ICAS), 2012, pp.1-12.

47. Caron, P. and Lavigne, O., "Recent Studies at ONERA on Super Alloys for Single Crystal Turbine Blades", Journal Aerospace Lab, Issue 3, November 2011, AL03-02, pp.1-14.

48. Reed, R. C., Huron, E. S., Hardy, M. C., Mills, M. J., Mantero, R. E., Portello, P. D. and Telesman, J., "Super Alloys", 2012, Wiley, ISBN: 1118516400.

49. Donachie, M. J. and Donachi, S. J., "Super Alloys: A Technical Guide", 2nd Edition, ASM International, 2002, ISBN 1615030646.

50. Watson, J. E., "Super Alloys: Production, Properties and Applications", Nova Science Publishers, 2011, ISBN 9781612095363.

51. Bowman, R., "Super Alloys: A Primer and History", Supplement to the Minerals, Metals and Materials Society's 9th International Symposium on Super Alloys, http://www.tms.org/meetings/specialty/superalloys 2000/superalloyhistory.html.

52. Zhang, H., Xu, Q. and Liu, B., "Numerical Simulation and Optimization of Directional Solidification Process of Single Crystal Superalloy Casting", Materials, Vol.7, No.3, 2014, pp.1625-1639.

53. Gell, M., Duhl, D. and Giamei, A., "The Development of Single Crystal Super Alloy Turbine Blades", Super Alloys, 1980, Proceedings of the Fourth International Symposium on Super Alloys, American Society of Metals, Metals Park, OH, 1980, pp.205-214.

54. Segersall, M., "Nickel-Based Single Crystal Super Alloys: The Crystal Orientation Influence on High Temperature Properties", Linkoping University Institute of Technology, Licentiate Thesis No.1568, March 2013.

55. Onyszko, A., Kubiak, K. and Sieniawski, J., "Turbine Blades of the Single Crystal Nickel Based CMSX-6 Super Alloy", Journal of Achievements in Materials and Manufacturing Engineering, Vol.32, Issue 1, January 2009, pp.66-69.

56. Zhang, R. L., Chen, L. N., Li, C. H., Wang, N., Lu, X. G. and Ren, Z. M., "Influence of Spiral Crystal Selector on Crystal Orientation of Single Crystal Super Alloy", Transactions of Nonferrous Metals Society of China, Vol.22, 2012, pp.1092-1095.

57. Esaka, H., Shinozuka, K. and Tamura, M., "Analysis of Single Crystal Casting Process Taking into Account the Shape of Pigtail", Journal of Materials Science and Engineering A, 2005, pp.413-414.

58. "Strengthened Super Alloy for Gas Turbine Blades", Metal Powder Report, Vol.47, Issue 10, October 1992, pp.24-28.

59. Suryanarayana, C., "Mechanical Alloying and Milling", Marcel Dekker, CRC Press, Taylor and Francis Group, 2004, ISBN 13:978-0-203-02064-7.

60. Park, L. J., Ryu, H. J., Hong, S. H. and Kim, Y. G., "Microstructure and Mechanical Behavior of Me-

chanically Alloyed ODS Ni-Base Super Alloy for Aerospace Gas Turbine Application", Advanced Performance Materials, Vol.5, 1998, pp.279-290.

61. Gell, M. and Thomas, K. M., "Development and Design of Directionally Solidified Eutectic Airfoils for Advanced Gas Turbine Engines", The American Society of Mechanical Engineers, Paper No. 76-GT-32, The Gas Turbine and Fluids Engineering Conference, New Orleans, La., March 21-25, 1976.

62. Dunlevey, F. M. and Wallace, J. F., "The Effect of Thermal Cycling on the Structure and Properties of a Co, Cr, Ni-TaC Directionally Solidified Eutectic Alloy", Transformations, Metallurgical Transactions, Vol.5, Issue 6, June 1974, pp.1351-1356.

63. Schilke, P. W., "Advanced Gas Turbine Materials and Coatings", GE Energy, GER-35696 (08/04).

64. Clemens, M. L., Price, A. and Bellows, R. S., "Advanced Solidification 31. Processing of an Industrial Gas Turbine Engine Component", JOM, March 2003, pp.27- 31.

65. Power, D. C., "Palladium Alloy Pinning Wires for Gas Turbine Blade Investment Casting", Platinum Metals Rev., Vol.39 (3), 1995, pp.117-126.

66. Visual Manufacturing Help: Investment Casting http://www.custompartnet.com/wu/investment_casting

67. Chyu, M. K. and Siw, S. C., "Recent Advances of Internal Cooling Techniques for Gas Turbine Airfoils", Journal of Thermal Science and Engineering Applications, Vol.5, June 2013, pp.021008-1 to 021008-12.

68. Siddique, W., "Design of Internal Cooling Passages: Investigation of Thermal Performance of Serpentine Passages", Doctoral Thesis, 2011, Division of Heat and Power Technology, Royal Institute of Technology, Stockholm, Sweden, Report 11/09, ISBN 978-91-7501-147-9.

69. "Turbine Blade Cooling", Ecole Polytechnique Federale de Lausanne, http://gtt.epfl.ch/page-63563-fr.html.

70. Al-Hadhrami, L. M, Shaahid, S. M, and Al-Mubarak, A. A., "Jet Impingement Cooling in Gas Turbines for Improving Thermal Efficiency and Power Density", www.intechopen.com.

71. Han, J. C., "Recent Studies in Turbine Blade Cooling", International Journal of Rotating Machinery, Vol.10 No.6, 2004, pp.443-457.

72. Ameral, S., Verstraete, T., Braembussche, R. V. and Arts, T., "Design and Optimization of the Internal Cooling Channels of a High Pressure Turbine Blade-Part I : Methodology", Journal of Turbomachinery, April 2010, Vol.132, pp.021013-1 to 021013-7.

73. Verstraete, T., Amaral, S., Braembussche, R. V. and Arts, T., "Design and Optimization of the Internal Cooling Channels of a High Pressure Turbine Blade-Part II : Optimization, Journal of Turbomachinery, April 2010, Vol.132, pp.021014-1 to 021014-9.

74. Zolfagharian, M. M., Zargarabadi, M. R., Majumdar, A. S., Valipoour, M. S. and Asadollahi, M., "Optimization of Turbine Blade Cooling Using Combined Cooling Techniques", Engineering Applications of Computational Fluid Mechanics, Vol.8, No.3, 2014, pp.462-475.

75. Gupta, S., Chaube, A. and Verma, P., Review on Heat Transfer Augmentation Techniques: Application in Gas Turbine Blade Internal Cooling", Journal of Engineering Science and Technology Review, Vol.5, No.1, 2012, pp.57-62.

76. Ligrani, P., "Heat Transfer Augmentation Technologies for Internal Cooling of Turbine Components of Gas Turbine Engines", International Journal of Rotating Machinery, Vol.2013 (2013), Article ID 275653, 32 pages.

77. Ligrani, P. M., Oliveira, M. M. and Blaskovich, T., "Comparison of Heat Transfer Augmentation Techniques", AIAA Journal, Vol.41, No.3, 2003, pp. 337-362.

78. Nathan, S., "Jewel in the Crown: Rolls Royces Single Crystal Turbine Blade Casting Foundry", 8th June 2015. https://www.theengineer.co.uk/jewel-in-the-crown-rolls-royce-single-crystal-turbine blade-casting-foundry

79. Felice, M., "Materials through the Ages: Materials for Aeroplane Engines" Materials World http: iom3.org/materialsworld-magazine/feature/2013/ may/09/materials- through-ages.

80. Xie, G. N., Sunden, B., Wang, L. and Utriainen, E., "Enhanced Heat Transfer on the Tip-Wall in a Rectangular Two-Pass Channel by Pin-Fin Arrays", Numerical Heat Transfer-Part A, 2009, Vol.52, pp.739-761.

81. Aerospace Engineering, "Jet-Engine Design: Turbine Cooling", May 1, 2013.

82. Volume 1. Performance Flight Testing Phase Chapter 7 Aero Propulsion, Feb 1991, USAF Test Pilot School, Edwards AFB, CA, USA.

83. Girardeau, J., Pailhas, J., Sebastian, P., Pardo, F. and Nadeau, J. P., "Turbine Blade Cooling System Optimization", Journal of Turbomachinery, Vol.135, Issue 6, 2013, pp.061020-1 to 061020-13.

84. "The Jet Engine", Rolls Royce, 1996, Revised 2005 ISBN: 0902121235, 978090212123 2.

85. Lakshminarayana, B., "Fluid Dynamics and Heat Transfer of Turbomachinery", 1996, John Wiley & Sons. ISBN: 0-471-85546-4.

86. Nasir, H., "Turbine Blade Tip Cooling and Heat Transfer", Ph. D. Dissertation in Mechanical Engineering Department, Louisiana State University, December 2004.

87. "6000-psi Waterjet Cutting Machines- Cuts Titanium Better than a Steel Blade or Drill", http://www.laser-cutting-online.com/waterjet-cutting-machines.html

88. Hashish, M., "Abrasive Waterjet Drilling of High Temperature Jet Engine Parts", Paper No. PUP2009-77365, pp. 65-73, ASME 2009 Pressure Vessels and Piping Conference.

89. Waterjet Drilling, http://www.laico.com/company-waterjet-drilling.html.

90. Wang, M. H., Zhu, D., Qu, N. S. and Zhang, C. Y., "Preparation of Turbulated Cooling Hole for Gas Turbine Blade using Electrochemical Machining", Key Engineering Materials, Vol.329, 2007, pp.699-704.

91. Coteata, M., Slatineanu, L., Dodun, O. and Ciofu, C., "Electrochemical Discharge Machining of Small Diameter Holes", International Journal of Material Forming, April 2008, pp.1327-1330.

92. Youssef, H. A., "Machining of Stainless Steels and Super Alloys: Traditional and Non-Traditional Techniques", John Wiley and Sons, 2016, ISBN 978-1-118-91956.

93. Brule, A., Deschamps, J. B., Marco, M. D., Richerzhagen, B. and Levine, H. H., "Laser Microjet for High Precision Drilling of Mechanical Devices such as Fuel Injection Nozzles", Proceedings of LPM2008, The 9th International Symposium on Laser Precision Microfabrication.

94. "GE, Synova and Makino Partner to Develop Advanced GT Manufacturing Machines", Modern Power Systems, 30 October 2014.

95. Clarke, D. R., Oechsner, M. and Padture, N. P., "Thermal Barrier Coatings for More Efficient Gas Turbine Engines", MRS Bulletin, Vol.37, October 2012, pp.891-898.

96. Sampath, S., Schulz, U., Jarligo, M. O. and Kuroda, S., "Processing Science of Advanced Thermal Barrier Systems", MRS Bulletin, Vol.37, October 2012, pp.903-910.

97. Padture, N. P., Gell, M. and Jordan, E. H., "Thermal Barrier Coatings for Gas Turbine Engine Applications", Science, Vol.296, A2 April 2002, pp.280-284.

98. Sourmail, T., "Coatings for Turbine Blades", University of Cambridge Website, June 5, 2006. http://www.msm.cam.ac.uk/phase-trans/2003/superalloys/coatings/index.html.

99. "High Temperature Coatings", Wadley Research Group, Department of Materials Science and Engineering, University of Virginia. http://www.virginia.edu/ms/research/wadley/high-temp.html

100. Schneibel, J. H., "Beyond Nickel-Base Superalloys", Proceedings of Processing and Fabrication of Advanced Materials XIII Conference, M. Gupta, T. S.

Srivatsan, CYH Lin, R. A. Varin Editors, Stallion Press, Singapore, 2005, pp.563-576.

101. Drawin, S. and Justin, J. F., "Advanced Lightweight Silicide and Nitride Based Materials for Turbo-Engine Applications", Journal Aerospace Lab, Issue 3, November 2011, Paper No.AL03-06, pp.1-13.

102. Schneibel, J. H., Kruzic, J. J. and Ritchie, R. O., "Development of Ultra-High Temperature Molybdenum Borosilicides", Proceedings of the 20th Annual Conference on Fossil Energy Materials, June 12-14, 2006, Oak Ridge National Laboratory.

103. Klemm, H., "Silicon Nitride for High Temperature Applications", Journal of the American Ceramic Society, Vol.93, 2010, pp.1501-1522.

104. "Flightpath 2050, Europe's Vision for Aviation", Report of the High Level Group on Aviation Research, European Commission, 2011, European Union, ISBN 978-92-79-19724-6.

105. Gardiner, G., "Aeroengine Composites, Part 1: The CMC Invasion", Composites World, August 2015, pp.38-41.

106. Wood, K., "Ceramic-Matrix Composites Heat Up", High Performance Composites, November 2013, pp.38-45.

107. Xu, L., Bo, S., Hongde, Y. and Lei, W., "Evolution of Rolls-Royce Air-Cooled Turbine Blades and Feature Analysis", Procedia Engineering, Vol.99, 2015, pp.1482-1491.

108. "GE Successfully Tests World's First Rotating Ceramic Matrix Composite Material for Next-Gen Combat Engine", GE Aviation, February 10, 2015 http://www.geaviation./press/military/military_20150210.html

109. Hirano, K., "Application of Eutectic Composites to Gas Turbine System and Fundamental Fracture Properties up to 1700°C", J. European Ceramic Society, Vol.25, 2005, pp.1191-1199.

110. Parlier, M., Valle, R., Perriere, L., Korinek, S. L. and Mazerolles, L., "Potential of Directionally Solidified Eutectic Ceramics for High Temperature Applications", Journal Aerospace Lab, Issue 3, November 2011, Paper Number AL03-07, pp.1-13.

111. Takahashi, K., Ando, K. and Nakao, W., "Crack-Healing Ability of Structural Ceramics and Methodology to Guarantee the Reliability of Ceramic Components", in the Book, Advances in Ceramics-Characterization, Raw Materials, Processing, Properties, Degradation and Healing, Edited by Costas Sikalidis, ISBN 978-953-307-504-4, August 1, 2011.

112. Raj, S. V., Singh, M. and Bhatt, R. T., "High Temperature Lightweight Self-Healing Ceramic Composites for Aircraft Engine Applications", NASA/TM 2014-218352, Glenn Research Center, October 2014.

113. Garvie, R. C., Hannink, R. H. J., and Pascoe, R. T., "Ceramic Steel?", Nature (London), Vol.258, 1975, pp.703-704.

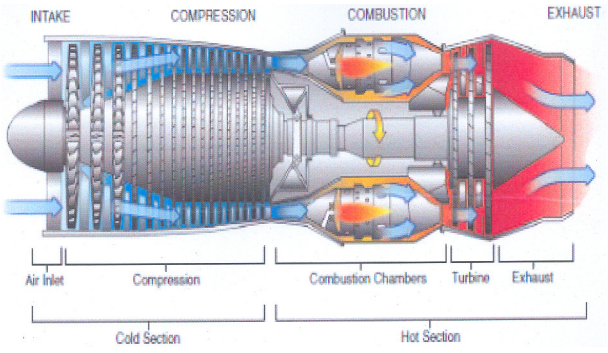

Fig.1 Major Components of a Gas Turbine Engine [Ref.3]

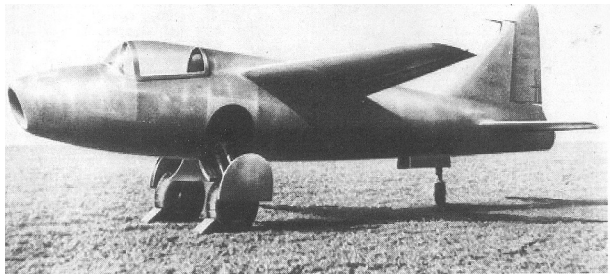

Fig.2 First Turbojet-Powered Aircraft - Ohain's Engine on He 178 [Ref.9]

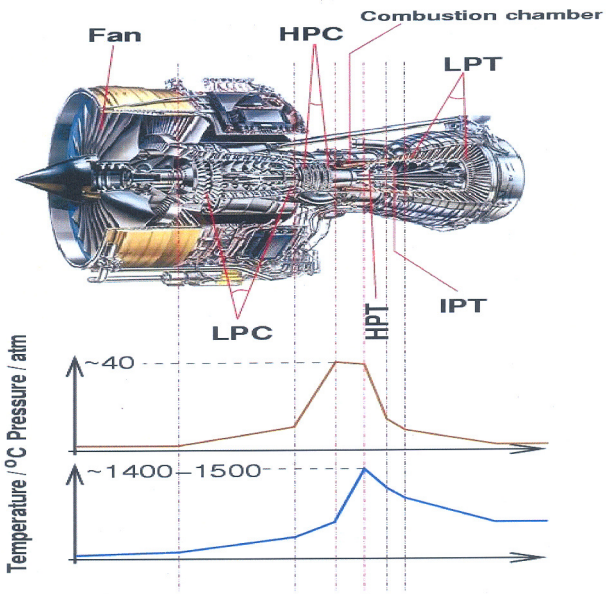

Fig.3 Pressure and Temperature Distribution Across a Roll Royce Trent 800 Engine [Ref.12]

Fig.5 Crack (Arrow) Observed in Trailing Edge Near Platform of Service-run Gas Turbine Blade [Ref.30]

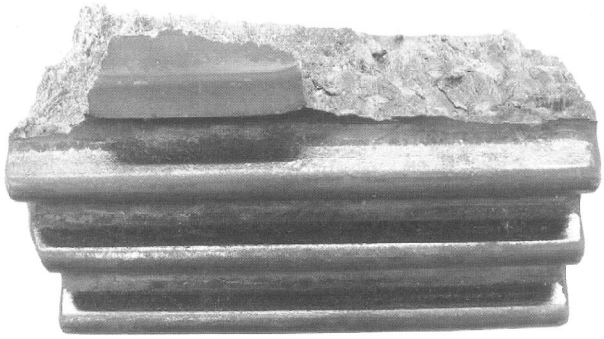

Fig.4 Fretting Failure at the Blade/Disk Attachment in the Fir Tree Joint [Ref.17]

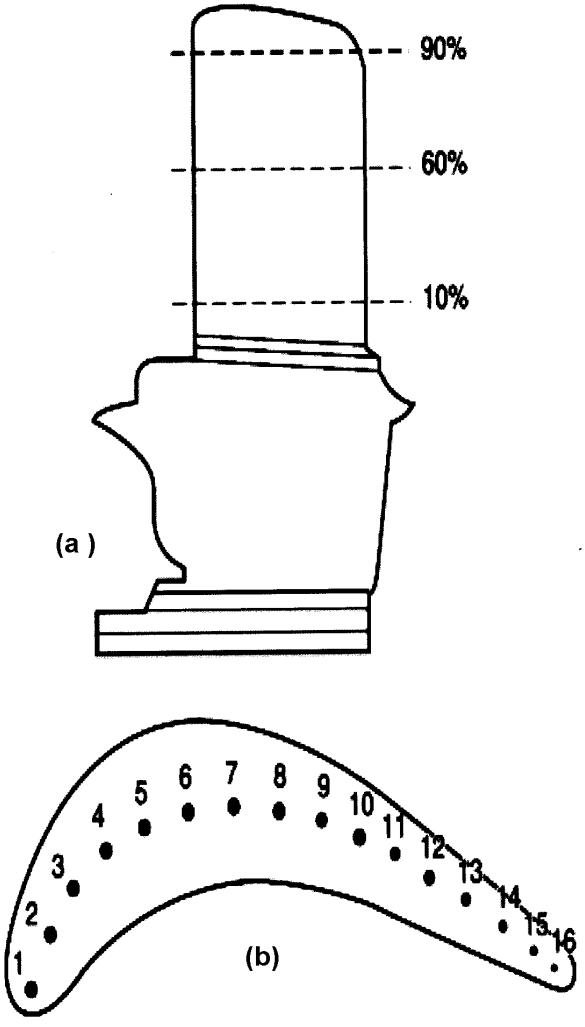

Fi.6 Schematic of First-Stage Gas Turbine Blade that Experienced Cracking After 32,000 h in Service. (a) Sectioning Planes at Three Locations on the Blade Airfoil (b) Cross-sectional View of the Blade Airfoil Showing the Cooling Holes and Numbering Sequence [Ref.31]

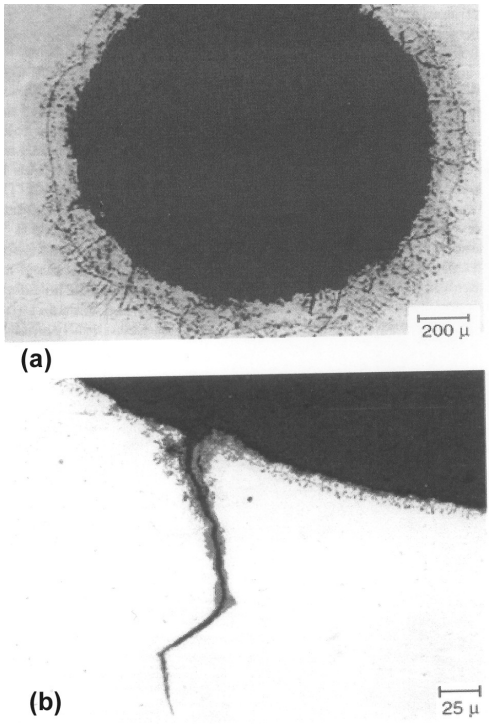

Fig.7 Oxidation and Cracking at Cooling Holes in a Turbine Blade (a) Trailing Edge cooling Hole Surface Showing Oxidation and Nitridation Attack on the Surface After 32,000 h of Operation (b) Crack found on the Surface of No.5 cooling Hole. Oxidation on the Crack Surface and Hole surface can be Noticed [Ref.31]

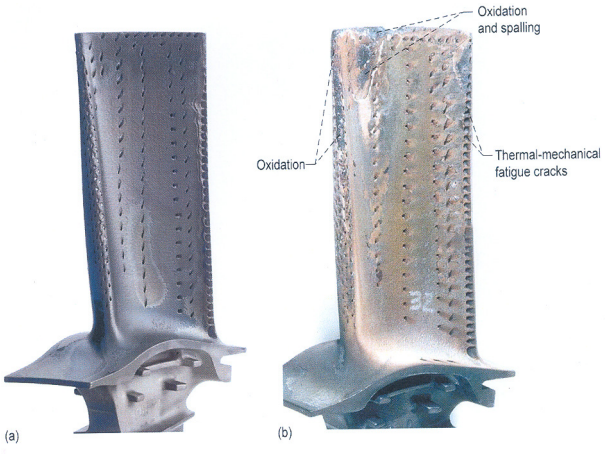

Fig.8 Comparison of Unfailed and Failed T-1 Turbine Blades Used in Study (a) Example of Unfailed T-1 Turbine Blade (b) Example of Failed T-1 Turbine Blade [Ref.13]

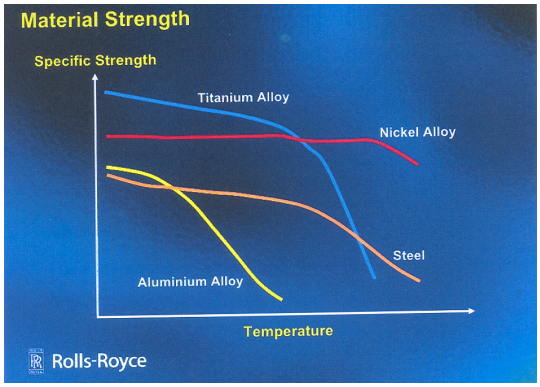

Fig.9 Variation of the Specific Strength of Important Alloys with Temperature [Ref.37]

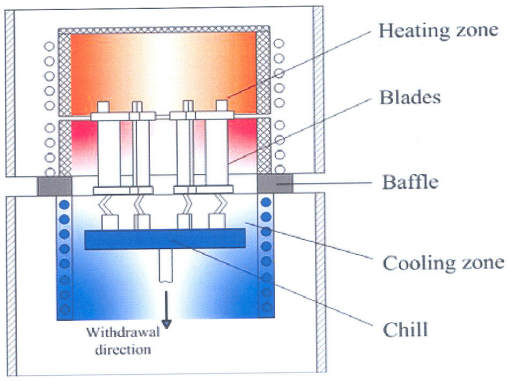

Fig.10 Directional Solidification of Super Alloy Blades [Ref.52]

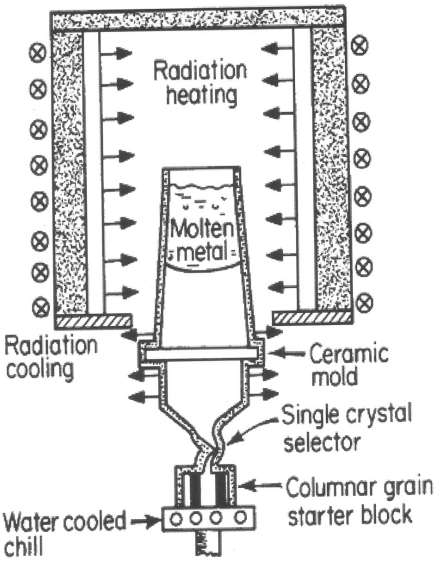

Fig.11 Single-Crystal Solidification Process for Casting Superalloy Turbine Blades to Eliminate Grain Boundaries [Ref.53]

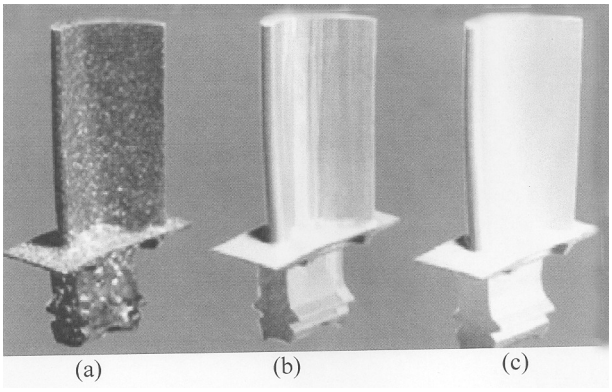

Fig.12 Nickle-Base Superalloy Turbine Blades Solidified as (a) Equiaxed Grains, (b) Columnar Grains, (c) a Single Crystal [Ref.37]

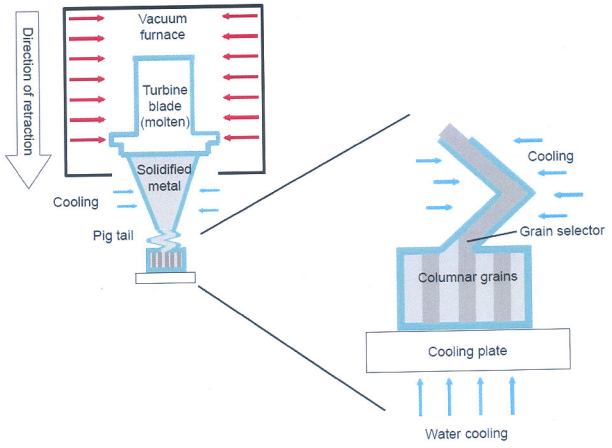

Fig.13 Investment Casting with Directional Solidification of a Turbine Blade in Single-Crystal Form [Ref.54]

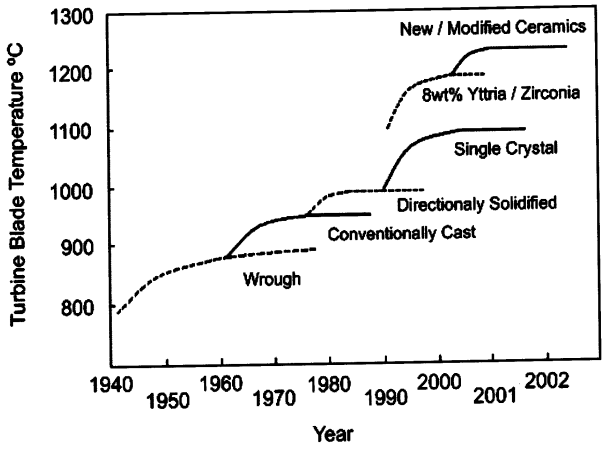

Fig.14 Chronological Increase in Operational Temperature of Turbine Components [Refs.55,56]

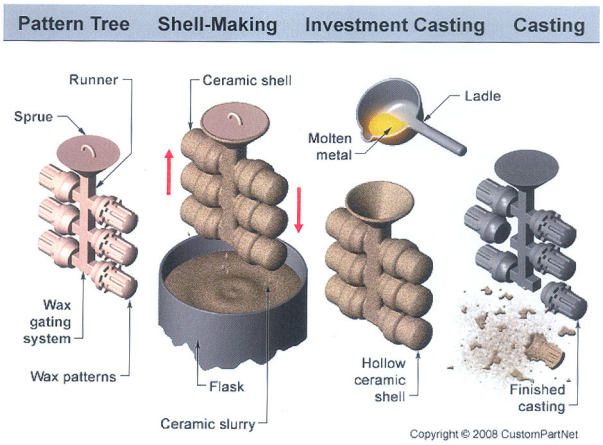

Fig.15 Major Steps Involved in Investment Casting [Ref.66]

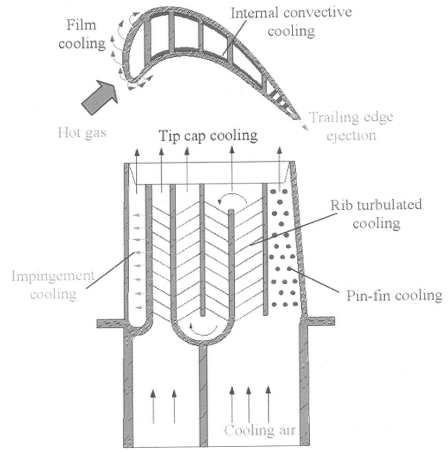

Fig.16 Passages Along the Length of a Blade Created for Blade Internal Cooling by Ceramic Cores [Ref.80]

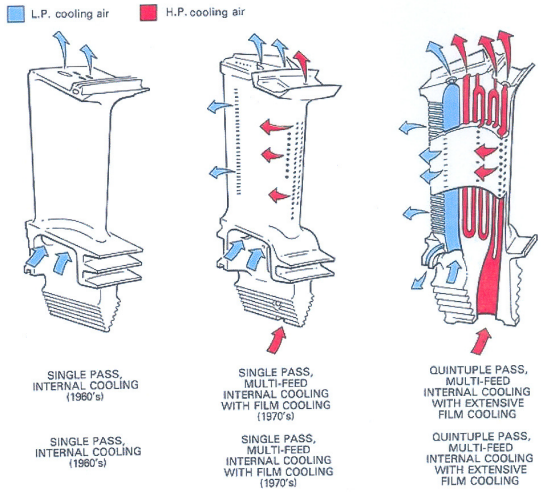

Fig.17 Single Pass and Multi-Pass Blade Internal Cooling [Ref.81]

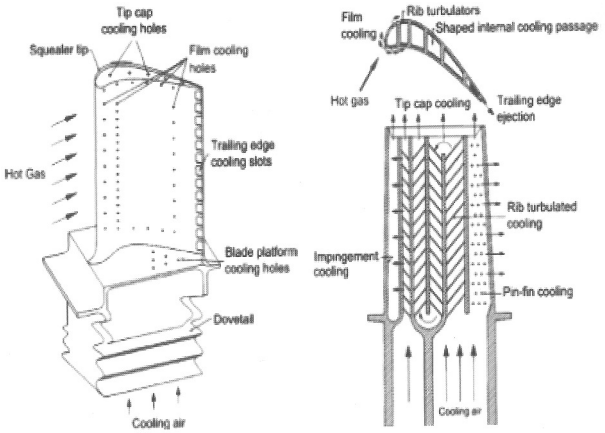

Fig.18 Schematic of Typical Gas Turbine Air Foil with Common Cooling Techniques [Ref.67]

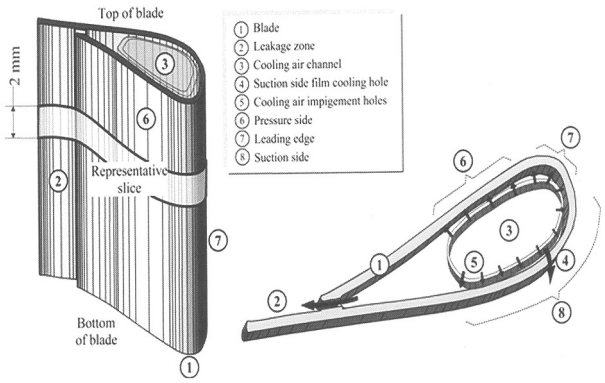

Fig.19 Turbine Blade and Representative Slice [Ref.83]

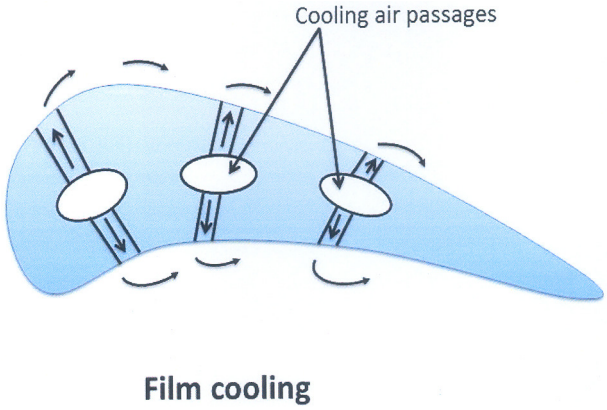

Fig.20 Film Cooling of Jet Engine Blade [Ref.84]

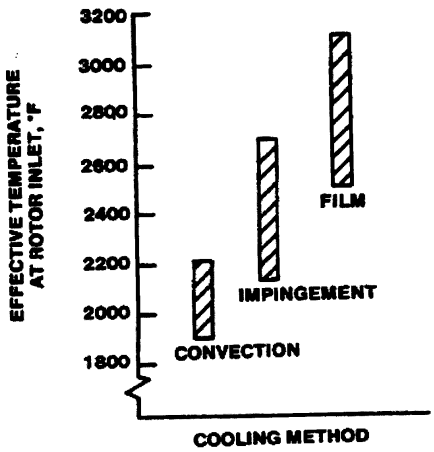

Fig.21 Relative Effectiveness of Turbine Blade Cooling Methods [Ref.82]

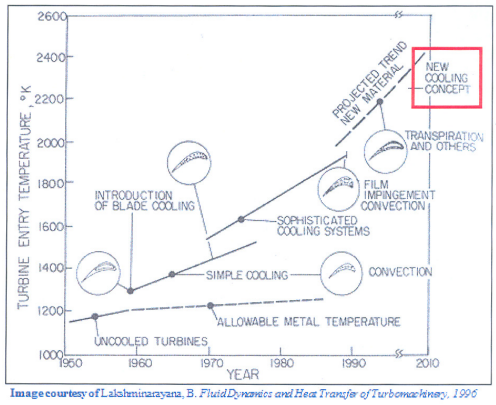

Fig.22 The Increase in TIT Over the Years Due to the Combined Effect of the Different Types of Cooling [Refs.84, 85]

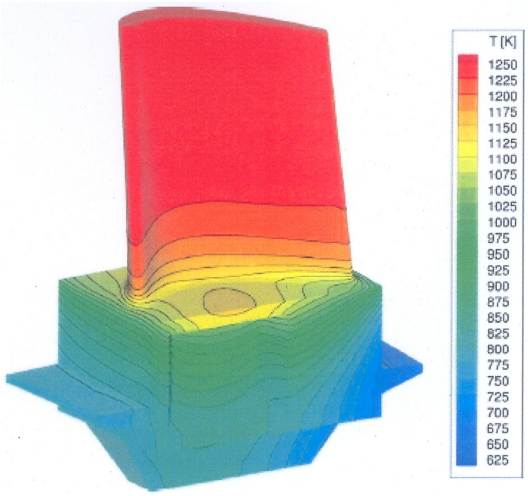

Fig.23 Temperature Distribution for a Blade Without Cooling Channels [Ref.72]

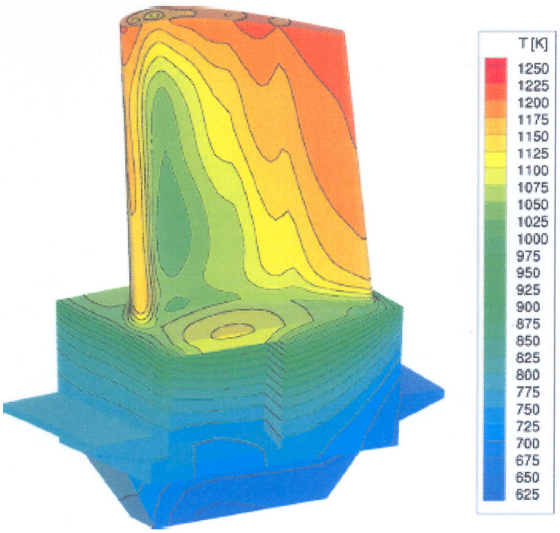

Fig.24 Temperature Distribution for a Blade With Cooling Channels [Ref.73]

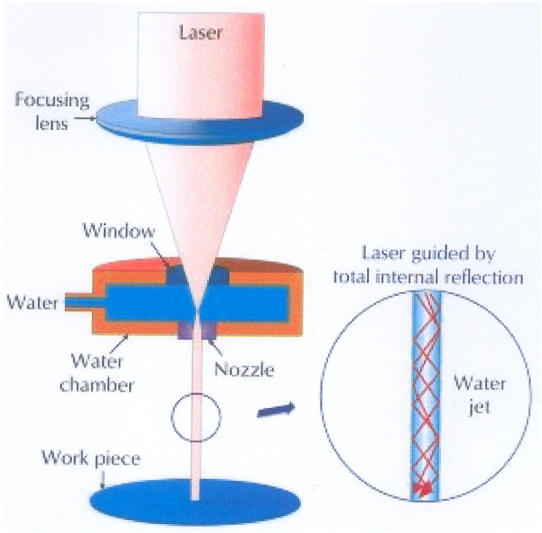

Fig.25 Laser Microjet Machining [Ref.93]

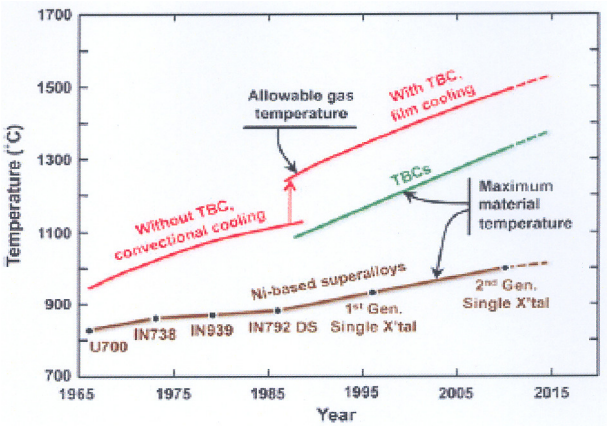

Fig.26 Comparison of Increases in TIT Due to Improvements in Super Alloy Chemistry with Increases in TIT Due to Internal Cooling and TBC [Ref.95]

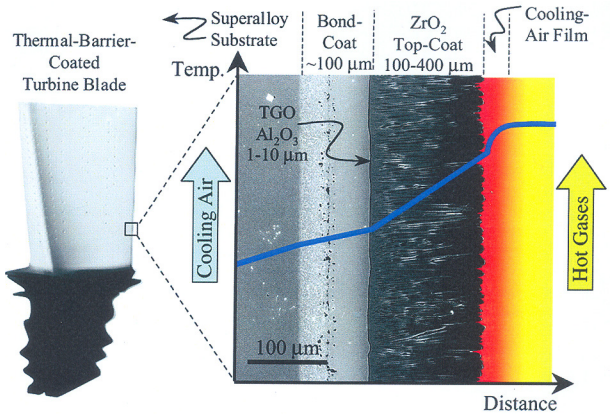

Fig.27 Temperature Drop Across the Different Layers of Thermal Barrier Coating [Ref.97]

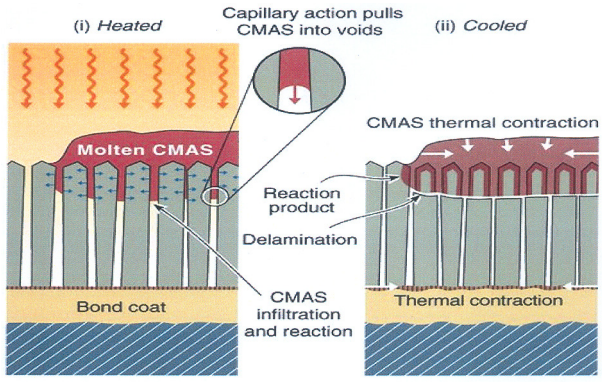

Fig.28 Molten CMAS Penetration Through TBC [Ref.99]

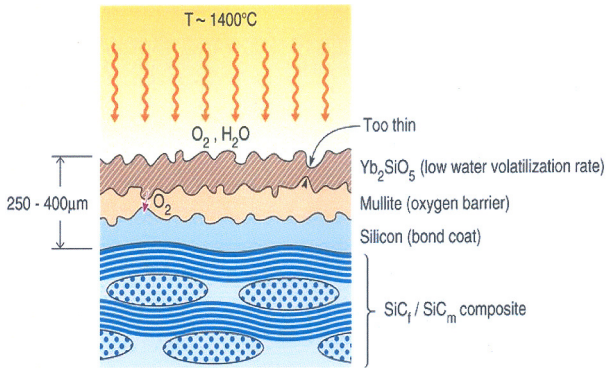

Fig.29 EBC for Ceramic or Ceramic Matrix Composite Blades [Ref.99]